Is chemical zonation in plutonic rocks driven by changes in source magma composition or shallow-crustal differentiation?

Drew S. Coleman[1,*], John M. Bartley[2], Allen F. Glazner[1], and Michael J. Pardue[1,†]
[1]*Department of Geological Sciences, CB#3315 Mitchell Hall, University of North Carolina, Chapel Hill, North Carolina 27599-3315, USA*
[2]*Department of Geology and Geophysics, University of Utah, Salt Lake City, Utah 84112-0111, USA*

ABSTRACT

Lithologic and magnetic-susceptibility mapping of the western Half Dome Granodiorite of the Tuolumne Intrusive Suite of California reveals seven km-scale lithologic cycles, each of which is bounded by a sharp west-dipping contact that is subparallel to the external contact of the pluton. Crosscutting relations indicate that the cycles become younger to the east. Each cycle is inferred to have been a zone of partial melt in which an eastern melt-depleted base grades westward to a melt-rich top now preserved as a leucocratic facies of the Half Dome Granodiorite. Sharp contacts between cycles may record freezing episodes when the rate of heat input into the growing pluton dropped below that required to maintain interstitial melt. Thus, the interstitial melt zone migrated with time and its size at any given time need not have differed greatly from the ~1 km thickness of the cycles. Cycles occur on the outer, older margins of the suite, and disappear toward the interior, younger intrusions. Inward disappearance of cycles likely reflects thermal maturation of the system such that melt was continuously present until the final migration of the solidus through the intrusive suite. Although the cycles span the compositional range from granodiorite to leucogranite, trace-element trends preserved in the cycles differ dramatically from those of both the Tuolumne Intrusive Suite and other Cretaceous zoned plutons of the eastern Sierra Nevada batholith. We suggest that (1) the compositional variations of the intrusive suite and the batholith reflect a signal from the source of the magmas, and (2) the geochemistry within the km-scale cycles reflects in situ crystal/liquid separation.

INTRODUCTION

Understanding magma chambers and how mapped plutons relate to them is fundamental to interpreting a broad range of issues in petrology, volcanology, tectonics, and seismology, including the geochemical evolution of the crust, links between plutonic and volcanic systems, and interpretation of seismic signals in magmatic areas (Daly, 1933; Lees, 2007; Lipman, 2007). Plutonic systems typically are chemically zoned at scales that range from individual mineral grains to entire intrusive suites. The zoning is commonly attributed to in situ magmatic differentiation and mixing at a variety of scales. At the largest scale, zoned intrusive suites share many common characteristics (e.g., see summaries in Pitcher and Berger, 1972; Paterson and Vernon, 1995). Furthermore, this map-scale zoning at least superficially resembles compositional zoning in voluminous ignimbrites (Hildreth, 1981, 2004); thus, a link between shallow plutonic rocks and silicic ignimbrites seems self-evident.

Textural and petrographic variants in zoned suites are usually mapped and interpreted as discrete pulses of magma intruded into a ballooning diapir (Pitcher and Berger, 1972; Bateman and Chappell, 1979), or as the products of in situ differentiation of a single magma body (Michael, 1984; Sawka et al., 1990; Hildreth, 2004). In the first interpretation, rock units defined by contacts represent the sizes and shapes of discrete magma batches that were fed into long-lived crustal magma chambers. In the second interpretation, the entire zoned pluton represents the fossil magma chamber, and mapped contacts are the result of post-intrusion differentiation. For example, high-silica igneous rocks that characterize the roof zones of many plutons (e.g., Michael, 1984; Johnson et al., 1989; Miller and Miller, 2002) are commonly interpreted to result from upward percolation of silicic liquids from a residual crystal mush (Baker and McBirney, 1985; Verplanck et al., 1999).

More recently, several groups have proposed that the geochemical zonation observed in individual plutons could be inherited from processes occurring during melt formation. Stevens et al. (2007) suggested that compositional variations observed in the S-type Cape Granite Suite (South Africa) could reflect variable entrainment of garnet and ilmenite, derived through biotite breakdown melting reactions, into the resultant leucogranite melts. Clemens et al. (2010) expanded this interpretation and asserted that high melt viscosities and slow diffusion rates require that most chemical variations preserved in plutonic and volcanic rocks must result from magma source processes rather than from shallow differentiation. Gray et al. (2008) proposed a different model with similar geochemical consequences, in which primary mafic magma mixes with variable-degree partial melts of previously intruded mafic material. Tappa et al. (2011) interpreted geochronologic data to suggest that the vertical zonation from shallow leucogranite to deep mafic granodiorite in the Rio Hondo pluton of the Latir volcanic field resulted from a change in the composition of magmas derived from their lower-crustal source. In that area, intrusion of the structurally high leucogranite preceded intrusion of deeper

*E-mail: dcoleman@unc.edu
†Present Address: Department of Environmental Engineering and Earth Sciences, Clemson University, 340 Brackett Hall, Clemson, South Carolina 29634-0919, USA

Geosphere; December 2012; v. 8; no. 6; p. 1568–1587; doi:10.1130/GES00798.1; 10 figures; 1 table; 1 supplemental table.
Received 18 February 2012 ♦ Revision received 13 August 2012 ♦ Accepted 13 August 2012 ♦ Published online 16 November 2012

granodiorites, ruling out the possibility that the former could have been derived through in situ differentiation of the latter.

Here we focus on variations within a well-dated pluton, the Half Dome Granodiorite (Khd—the map unit designation) of the Tuolumne Intrusive Suite (TIS), Sierra Nevada batholith, California, to evaluate the origin of compositional variations within the unit and the implications for variations in the suite as a whole. We focus on the role of crystal-liquid separation in the Half Dome Granodiorite and the Tuolumne Intrusive Suite (TIS) to address conflicting interpretations of that rock unit. We have suggested that magma accumulation rates were too slow to permit significant in situ fractionation (Coleman et al., 2004; Glazner et al., 2004; Gray et al., 2008), but several recent investigations have asserted that crystal fractionation was indeed significant in this suite (Žák and Paterson, 2005; Solgadi and Sawyer, 2008; Economos et al., 2010; Memeti et al., 2010). We present new field and geochemical data from the Half Dome Granodiorite that we interpret in combination with published geochemical data from previous studies, and new geochemical data for leucogranites in the Sierra Nevada batholith to permit better understanding of the relationships between high-silica facies in the Half Dome unit, high-silica granites, and high-silica rhyolites.

GEOLOGIC SETTING

The Sierra Nevada Range of California exposes the plutonic roots of a portion of the Mesozoic arc constructed along the western margin of North America (Fig. 1). Granodioritic and granitic rocks dominate present exposures in the batholith, but sparse mafic and high-silica rocks are also exposed (Bateman, 1992). Intermediate composition rocks form huge (>1500 km^2)

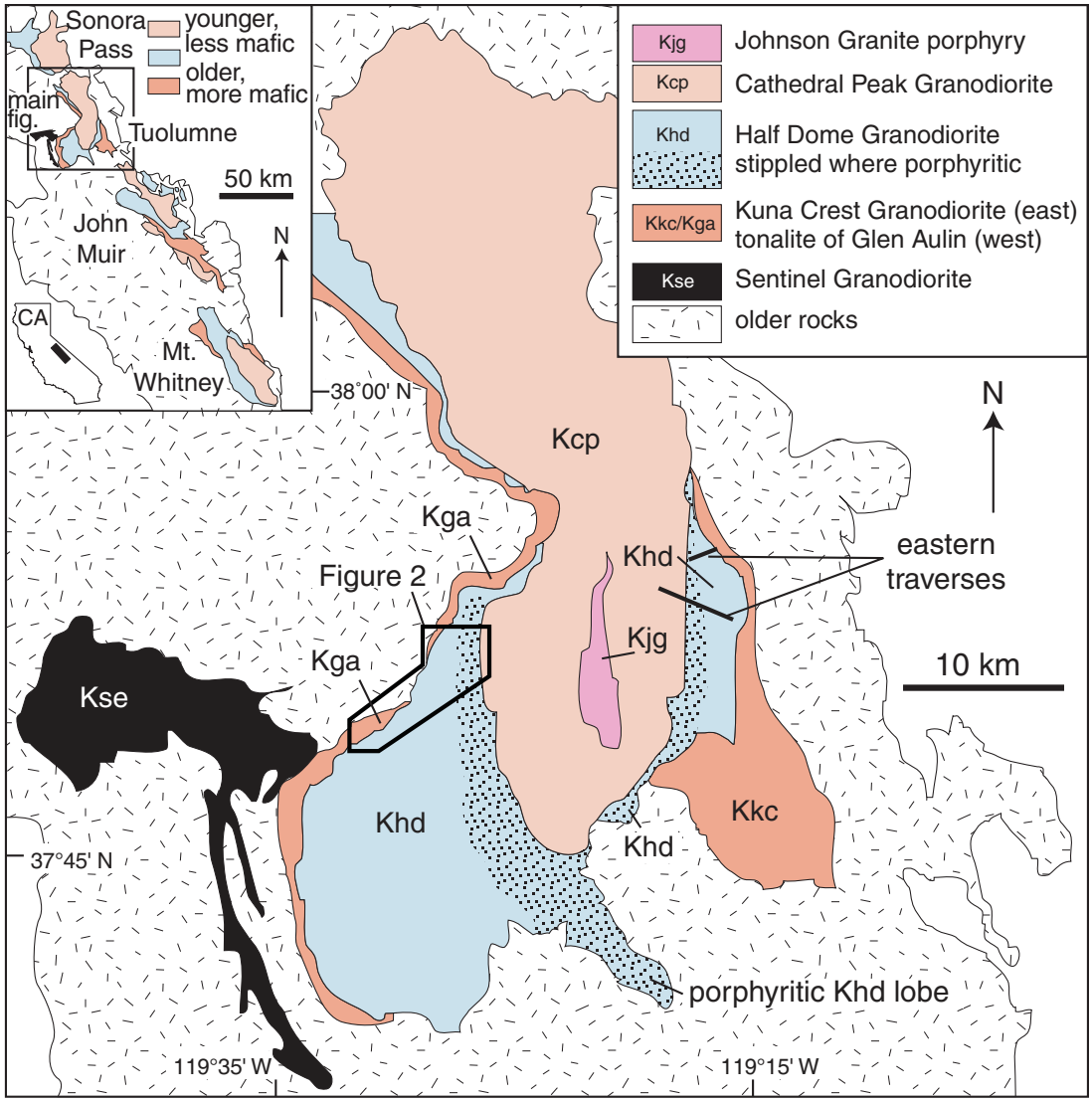

Figure 1. Simplified geology of the Tuolumne Intrusive Suite after Bateman (1992). Inset shows the location of the Tuolumne and other Sierra Crest zoned intrusive suites. Locations of detailed map (Fig. 2) and eastern magnetic susceptibility traverses are indicated. Geochronologic data (Coleman et al., 2004; Memeti et al., 2010) demonstrate that the suite was assembled incrementally between ~95 and 85 Ma. Individual map units are also diachronous. Most contacts between map units are gradational, although they are locally sharp. The lobe of porphyritic Half Dome Granodiorite (Khd) (Economos et al., 2010) discussed in text is indicated.

individual plutons and zoned intrusive suites of similar size (Bateman, 1992). High-silica rocks are generally limited to aplite dikes (Glazner et al., 2008) and sparse leucogranite plutons (Bateman, 1992; Wenner and Coleman, 2004). Geochemical data from the aplite dikes demonstrate that they are not intrusive equivalents of high-silica volcanic rocks (Glazner et al., 2008). However, limited data from leucogranites suggest that they are chemically distinct from aplites and that they represent a potential end member, if intermediate composition plutons and zoned intrusive suites originated by mixing between this silicic composition magma and mafic magma (Sisson et al., 1996; Wenner and Coleman, 2004).

The Cretaceous Tuolumne Intrusive Suite is one of several large, zoned intrusive complexes exposed in the Sierra Nevada batholith (Bateman, 1992; Fig. 1). Sierran zoned intrusive suites such as the Tuolumne Intrusive Suite and the John Muir Intrusive Suite (Bateman, 1992; Davis et al., 2012) share many characteristics that are typical of zoned suites worldwide and include a temporal and spatial progression from older, outer tonalitic units inward to younger granodioritic to granitic rocks. Geochronologic data show that Sierran zoned suites were intruded during the Sierra Crest Magmatic Event (~98–86 Ma; Coleman and Glazner, 1997) and that the Tuolumne and John Muir suites intruded over comparable durations between ~95 and 85 Ma (Kistler and Fleck, 1994; Mahan et al., 2003; Coleman et al., 2004; Memeti et al., 2010; Davis et al., 2012).

The concentrically arranged map units identified in the Tuolumne Intrusive Suite by Bateman and Chappell (1979) are distinguished by the proportion of mafic minerals and the presence or absence of euhedral hornblende phenocrysts and K-feldspar megacrysts. Contacts between map units are most commonly gradational, though sharp contacts are locally observed (Bateman et al., 1983). Half Dome Granodiorite is distinguished from the outer tonalites (Glen Aulin, Glacier Point, and Kuna Crest) by the presence of cm-scale euhedral hornblende phenocrysts. Porphyritic Half Dome Granodiorite is distinguished by the appearance of poikilitic K-feldspar phenocrysts 2–4 cm across, and the Cathedral Peak Granodiorite contact is marked by an increase in K-feldspar size to megacrysts 10 cm in length, which appear over a very short distance and locally define a sharp boundary (Johnson and Glazner, 2010). The mapped contact of the Cathedral Peak pluton with the porphyritic Half Dome pluton is drawn to coincide with the inward appearance of the largest K-feldspar megacrysts in the Tuolumne Intrusive Suite (Bateman and Chappell, 1979).

The textural changes that define the map units of the Tuolumne Intrusive Suite do not correlate closely with changes in composition or isotope geochemistry. Excluding the late Johnson Granite Porphyry, most of the bulk-compositional differences (specific gravity, modal mineralogy, and isotope geochemistry) occur within 2 km of the outermost contact of the intrusive suite (Kistler et al., 1986; Bateman, 1992; Gray et al., 2008; Mills et al., 2009). Chemical variations within the equigranular Half Dome map unit span the entire compositional range of the Tuolumne Intrusive Suite (Gray et al., 2008). Likewise, isotopic ratios change significantly between the outermost tonalites and the equigranular Half Dome Granodiorite, but there is little spatially coherent variation in the isotope geochemistry of the porphyritic Half Dome and Cathedral Peak plutons (Kistler et al., 1986; Coleman and Glazner, 1997; Gray et al., 2008).

Coleman et al. (2005) mapped petrographic variations within Half Dome Granodiorite. They documented km-scale cyclic changes in petrography and magnetic susceptibility within the equigranular phase of the granodiorite and speculated that each cycle might represent the spatial scale of interconnected melt within the Tuolumne Intrusive Suite. Field data suggest that the age progression of the cycles mimics the well-documented age progression of the Tuolumne Intrusive Suite as a whole in younging toward the center of the Suite (Coleman et al., 2005).

Several more recent studies highlight petrographic and geochemical variations within the Half Dome Granodiorite and other map units of the Tuolumne Intrusive Suite. Memeti et al. (2010) mapped and dated four lobes of the Tuolumne Intrusive Suite intrusive rocks that extend outward from the main part of the suite into country rocks. Economos et al. (2010) examined the petrographic and geochemical variation in one of these lobes extending from the southeast margin of the Half Dome Granodiorite (Fig. 1). The limited age range within individual lobes (<1 Ma), and geochemical variations in the Half Dome lobe led these authors to conclude that they intruded quickly and thus provide frozen snapshots of internal differentiation within the Tuolumne magma system. These authors also asserted that similar variation was not preserved within the main body of the Tuolumne Intrusive Suite and speculated that the lack of such variation reflected cm- to km-scale mixing within the main body. However, the petrographic and chemical variations they describe are similar to the cycles preserved in the main body of equigranular Half Dome Granodiorite (Coleman et al., 2005). The only distinctions between lobes and cycles are outcrop geometry (isolated lobes versus tabular cycles) and the fact that whereas lobes apparently preserve a single differentiation event, cycles preserve evidence for multiple discrete differentiation events.

METHODS

In addition to traditional geologic mapping at 1:10,000, we mapped variations in magnetic susceptibility of the western Half Dome Granodiorite between Tenaya Lake and the east end of Yosemite Valley (Figs. 2 and 3). This work expanded significantly on our preliminary mapping in the area (Coleman et al., 2005). Magnetic susceptibility of the rocks was measured using a hand-held ZH Instruments model SM-30 susceptibility meter at nearly 1500 stations throughout the map area (see Supplemental Table 1[1]). Stations were located on unweathered, glacially polished outcrop where the polish had either flaked off or the surface was jointed to expose unpolished faces. Early attempts to measure the polished surfaces themselves yielded unacceptably scattered results from individual sites. At each station, susceptibility was measured nine times at different spots within a small area—ideally, on a 3 × 3 grid 1 m on a side. For most stations we were able to restrict measurements to within several square meters, but at some locations weathering forced us to expand the analysis zone. Whenever possible, we measured multiple surfaces in different orientations to average susceptibility anisotropy, if any. We also tried to measure visually homogeneous sites, and avoided obvious heterogeneity (e.g., schlieren and enclaves) and alteration (e.g., oxidation).

Three different units were used to measure the magnetic susceptibility (two SM-30s and one GMS-2). The units were carefully calibrated against each other by measuring identical points on a surface, and all data are reported using a correction to the most frequently used instrument (a UNC SM-30; Supplemental Table [see footnote 1]). Magnetic susceptibility variations are presented as a surface constructed in ESRI(R) ArcMap™ 9.2 as a third-order local polynomial using the 100 nearest neighbors. This method was chosen by trial and error and seems to smooth the data effectively while still honoring local variability.

Several magnetic-susceptibility transects were completed through the eastern exposures

[1]Supplemental Table. Excel file of in situ magnetic susceptibility measurements in the Tuolumne Intrusive Suite. If you are viewing the PDF of this paper or reading it offline, please visit http://dx.doi.org/10.1130/GES00798.S1 or the full-text article on www.gsapubs.org to view the Supplemental Table.

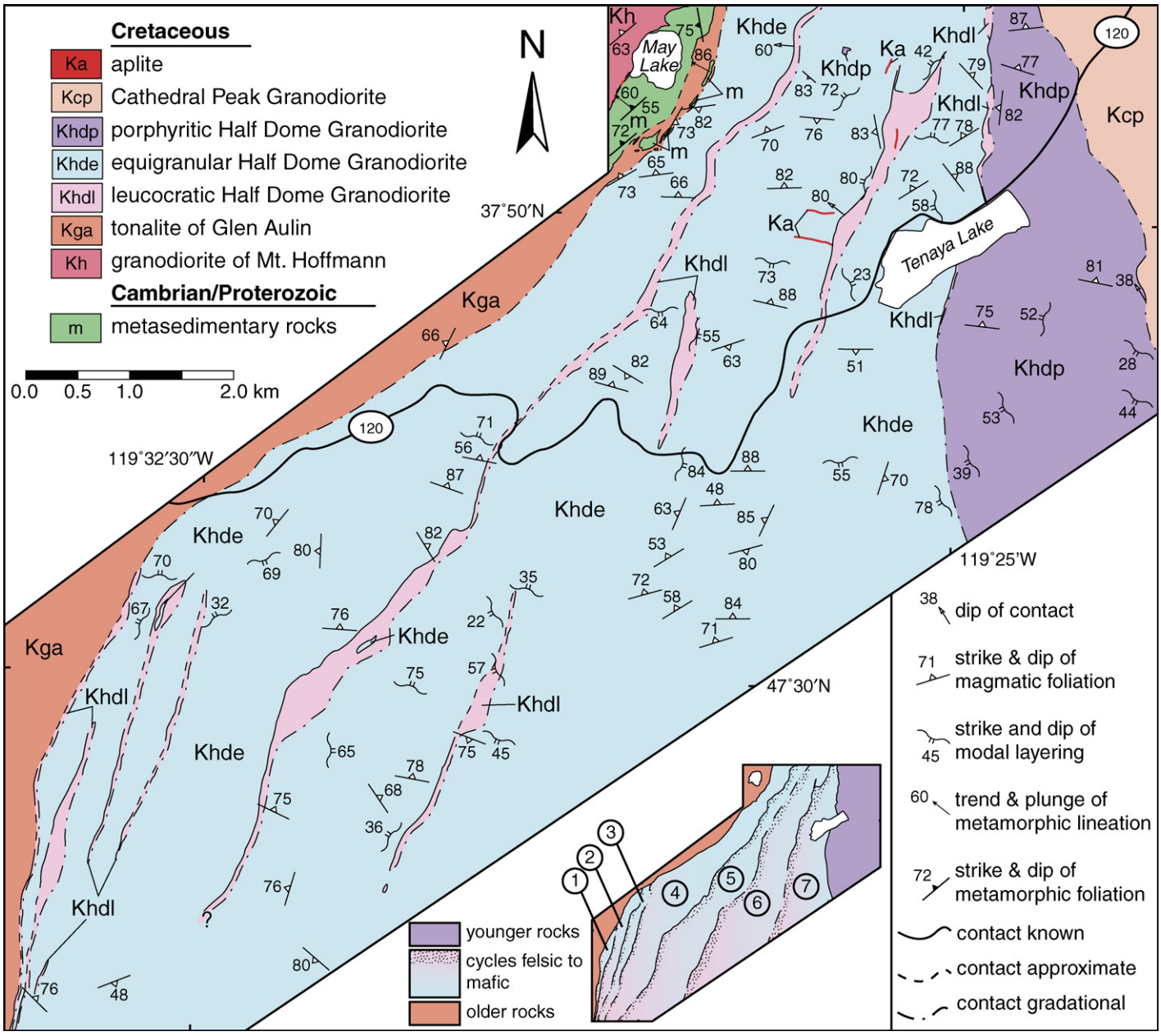

Figure 2. Geologic map of the western Half Dome Granodiorite (Khd). Geology of wall rocks at May Lake from Taylor (2004). The westernmost Khd is characterized by at least seven repetitious cycles with sharp western contacts between granodiorite and a leucocratic facies with large euhedral hornblende crystals characteristic of the granodiorite (inset). To the east, these leucocratic zones are gradational back into normal, and sometimes more mafic, Khd. Sharp contacts between the leucocratic facies and "normal" Khd are ubiquitously on the western contact and are steeply dipping to the west. In several locations, the leucocratic facies intrudes the granodiorite to the west as thin dikes (mapped as aplite). Foliation, defined by hornblende, strikes at high angle to the mapped contacts as it does elsewhere in the Tuolumne Intrusive Suite (TIS) (Bateman et al., 1983).

of the Half Dome Granodiorite. The transects were oriented at high angles to external contacts in an effort to determine if cyclic variations in susceptibility recognized in the western part of the pluton were also present in the east. Data collection methods were identical to those described for the map area.

Samples for geochemical analysis were collected at ten magnetic susceptibility sites through the southeasternmost cycle in Figure 2. Six additional samples were collected from other locations in the mapped area. Samples were crushed with a jaw crusher to centimeter-sized chips, then powdered in an alumina-ceramic shatterbox. All chemical analyses were completed by Actlabs (Ontario, Canada). Samples were dissolved by fusion in a lithium metaborate/tetraborate mixture; major elements and Ba, Sr, Y, Zr, Sc, Be, and V were analyzed by inductively coupled plasma–optical emission spectroscopy (ICP-OES), with remaining

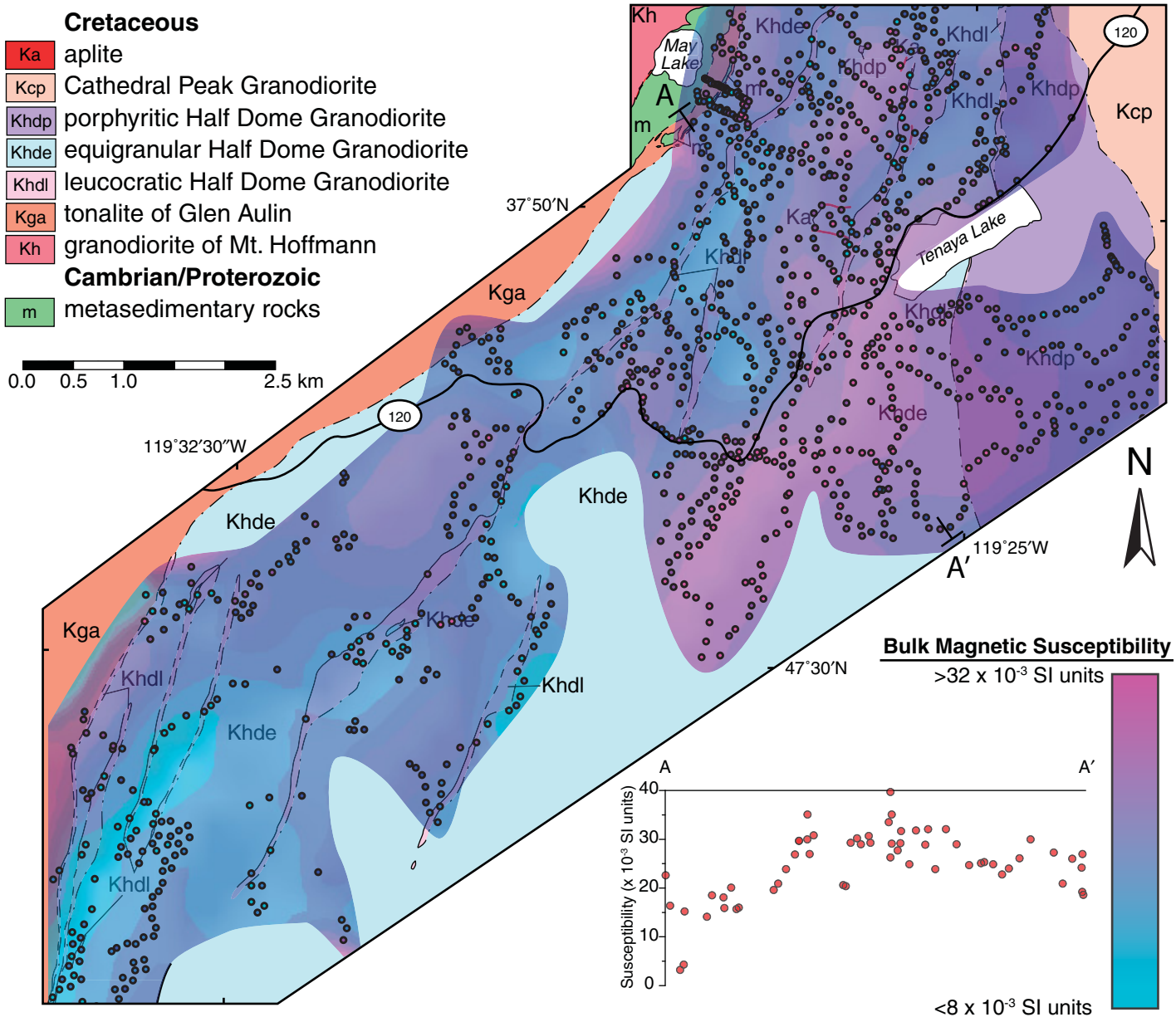

Figure 3. Magnetic susceptibility map of the western Half Dome Granodiorite (Khd). Map area is the same as that shown in Figure 2. Inset shows magnetic susceptibility along traverse A–A′ with data projected from 150 m from either side of the traverse line. Magnetic susceptibility mapping provides a technique to quantify petrographic variation in the field. Low magnetic susceptibility regions correlate with the mapped leucocratic facies. See text for discussion.

trace elements analyzed by inductively coupled plasma–mass spectrometry (ICP-MS).

In order to expand the database for leucogranites from the Sierra Nevada batholith, eleven samples were collected from four mapped leucogranites. Sampled units included the Johnson Granite Porphyry (Bateman, 1992), and the Bullfrog, Red Mountain Creek, and Taboose granites (Moore, 1963). With the exception of the Jurassic Red Mountain Creek pluton, leucogranites sampled are Cretaceous in age. The Johnson Granite Porphyry is ~85 Ma (Coleman et al., 2004) and is the youngest exposed unit in the Tuolumne Intrusive Suite. The Bullfrog pluton is ~103 Ma (Chen and Moore, 1982) and is one of the ~100 Ma plutons that crop out between the John Muir Intrusive Suite to the north and the Mount Whitney Intrusive Suite to the south (Fig. 1, inset; Moore, 1963). The Taboose and Red Mountain Creek granites are adjacent to each other on the SE side of the John Muir Intrusive Suite. The Red Mountain Creek Granite is cut by the 148 Ma Independence dike swarm (Moore, 1963) and is likely Jurassic. The Taboose granite is not cut by the dike swarm and is therefore interpreted to be Cretaceous (Bartley et al., 2012). Samples were selected based on spatial distribution, both vertically and horizontally, and textural contrasts. Care was taken to only choose the freshest samples for geochemical analysis. Analysis of leucogranites followed the same methods outlined for the samples collected from the cycle.

RESULTS

Mapping and Magnetic Susceptibility Survey

Geologic mapping revealed that the petrography and magnetic susceptibility of equigranular Half Dome Granodiorite are heterogeneous and that the heterogeneities form a coherent pattern. The pattern repeats at least seven times between the contacts with the tonalite of Glen Aulin and the porphyritic Half Dome Granodiorite, and we refer to each repetition as a "cycle." Portions of the easternmost cycles in Figure 2 are the same as those mapped by Coleman et al. (2005). An individual cycle is characterized by a sharp eastern contact with the adjacent cycle and a gradational westward decrease in the abundance of mafic minerals (Fig. 2). The two easternmost and youngest cycles are the thickest and most completely exposed. Cycles near the outer margin of the Half Dome pluton are thin and more poorly developed than those toward the mapped contact with the porphyritic facies of the pluton (Fig. 2). Similar cyclic variations were not found within either the porphyritic Half Dome Granodiorite or the Cathedral Peak Granodiorite.

Cycles are dominated by outcrop of Half Dome Granodiorite with color index (CI—defined as the volume percentage of dark minerals, dominantly hornblende and biotite) ~5–15 (Bateman, 1992) that we refer to as "normal" Half Dome Granodiorite. In Figure 2, a zone of leucocratic Half Dome pluton was mapped where we visually estimated the CI to be less than 2. Kistler (1973) mapped several of the westernmost leucocratic zones as aplite. However, the rocks are medium-grained leucogranite that contains the large euhedral hornblende phenocrysts that characterize Half Dome Granodiorite, and the mapped bodies characteristically have a sharp western contact but a diffuse eastern contact (Figs. 2 and 4C).

As noted by Bateman et al. (1983), Half Dome Granodiorite is characterized by a foliation defined by hornblende that dips steeply and strikes at high angles to unit contacts and to internal contacts within the granodiorite (Fig. 2). Modal layering (also referred to as sheets or schlieren, but we prefer to use a nongenetic term) is locally present throughout the map area and varies both in strike and dip much more than the foliation. Modal layers form semicontinuous alternating bands of mafic and felsic minerals, and locally ladder dikes (Reid et al., 1993).

Individual magnetic susceptibility measurements varied from maximum values in excess of 4×10^{-2} to less than 1×10^{-2} SI units (Supplemental Table [see footnote 1]). Such high values imply that the bulk magnetic susceptibility is dominated by a very high-susceptibility phase, which almost certainly is magnetite (Hunt et al., 1995). The standard deviation of susceptibility measurements at individual stations was typically 1%–5% of the mean, but at some stations it approached 50%. Such large variations appear to reflect mineralogical heterogeneity. Qualitatively, magnetic susceptibility (and thus magnetite abundance) correlates with the abundance of mafic minerals in the rock. Low magnetic susceptibility regions correlate with bodies of leucocratic Half Dome Granodiorite (Fig. 3). Across a cycle, magnetic susceptibility increases sharply (from values typically $<1 \times 10^{-2}$ to $>2.5 \times 10^{-2}$ SI units) westward across contacts between leucocratic and normal Half Dome, then slowly decreases toward the next body of leucocratic Half Dome. Cyclic variations in susceptibility detailed in the western portion of Half Dome Granodiorite are also evident in traverses through the eastern portion (Fig. 5), and, as in the western cycles, the most completely developed and well-defined cycle is preserved near the boundary between the equigranular and porphyritic facies of the Half Dome Granodiorite.

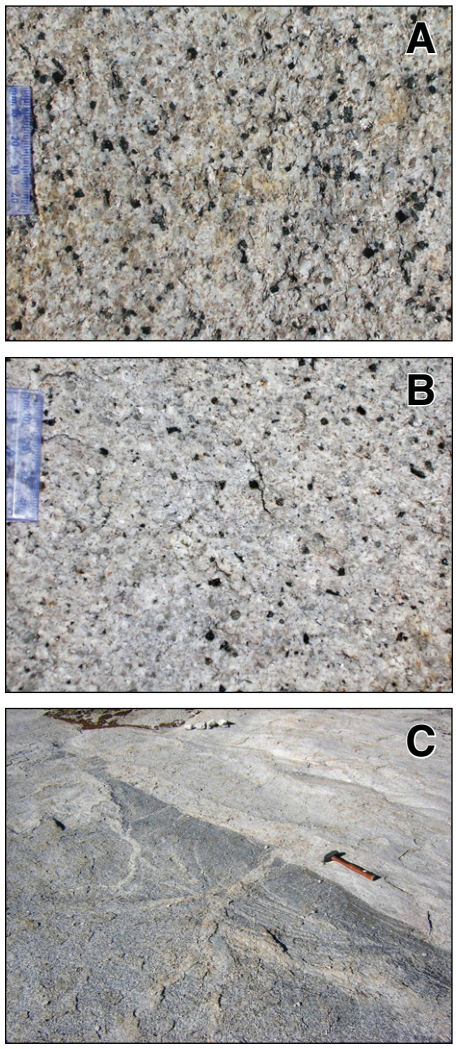

Figure 4. Photos of the Half Dome Granodiorite (Khd). (A) "Normal" Khd with high CI (color index) and abundant cm-scale, euhedral hornblende crystals. (B) Leucocratic facies of the Khd exposed only in thin discontinuous bodies. Although this facies has a distinctly lower CI than the normal granodiorite, it is still characterized by cm-scale euhedral hornblende crystals. (C) Sharp western contact of the leucocratic facies of the Khd with adjacent "normal" granodiorite. A thin dike of the leucocratic facies cuts the facies to the west. The eastern contact of these bodies of the leucocratic facies is everywhere gradational within the map area.

Geochemistry

The geochemistry of the cycle sampled varies predictably with horizontal distance from the eastern contact (Table 1; Fig. 6). Only the most silicic sample falls significantly off of spatial trends defined by the other samples. From east to west, SiO_2 and K_2O concentrations generally increase and concentrations of Al_2O_3, MgO, Fe_2O_3t, and CaO generally decrease. The most silicic samples from the cycle overlap in major oxide concentrations with leucogranites and aplites (Fig. 7A). However, they are characterized by significant depletion in Y, Sr, and the middle rare earth elements (MREE—shown as [Gd]) relative to lower silica portions of the cycle (Fig. 8A), and are therefore, much more similar to aplite (cf. Glazner et al., 2008) than the leucogranites.

Bulk compositions of the analyzed samples correlate with magnetic susceptibility (Fig. 9): high Fe sites have significantly higher bulk susceptibility than low Fe sites. The correlation suggests that susceptibility mapping can be a fast and effective tool for quantifying rock variations in the field, if the outcrop is sufficiently fresh, magnetite is present, and the Fe-oxide mineralogy does not vary owing to variations in oxidation state.

Leucogranites are characterized by high SiO_2 (72–78 wt%) and low MgO (<0.5 wt%; Table 1; Fig. 7A). More generally, their major-element compositions resemble high-silica rocks worldwide. The major oxide compositions of the leucogranites lie along continuations of trends defined by rocks with <72 wt% SiO_2 (Fig. 7B). At low SiO_2, the leucogranites overlap with the most silicic rocks in the Tuolumne Intrusive Suite and elsewhere, and at high SiO_2,

they overlap with the compositions of aplites. However, leucogranites and aplites differ significantly in their trace-element signatures. For example, concentrations of high field strength elements (HFSEs), MREEs, and Y are distinctly higher in leucogranites than aplites. Similarly, the extreme depletion in Y in the aplites yields very low Y/Sr. Whereas the major oxide chemistry of leucogranites is indistinguishable from that of the leucocratic facies of Half Dome Granodiorite (Fig. 7A), the trace-element geochemistry of the leucogranites distinguishes the two rock types (Fig. 8A).

DISCUSSION

Here we examine the geochemical trends defined by cycles, lobes, aplites, and leucogranites and compare these trends to geochemical trends defined by the Tuolumne Intrusive Suite and other zoned plutons of the Sierra Crest Magmatic Event to evaluate origins of the chemical variation. Next, we compare these results to data for volcanic rocks preserved in the Sierran arc. We use these data to evaluate hypotheses for the origin of chemical variation in the volcanic rocks and plutonic/volcanic rock links.

Geochemistry and Origin of the Cycles

With the exception of the most silicic sample, the geochemical data for the cycle span the same compositional range as published data for Half Dome Granodiorite (Figs. 6 and 7B; Bateman et al., 1984; Gray et al., 2008), and scatter about the median of the published analyses. Three alternative interpretations of the cycles must be evaluated in light of field, petrographic, and geochemical data. First, the cycles could represent normal Half Dome Granodiorite intruded by aplites (Kistler, 1973). Second, the cycles could reflect incremental assembly characterized by cyclic temporal variation of the composition of magma added to the Tuolumne Intrusive Suite. Finally, the cycles could represent in situ crystal/liquid separation. The third hypothesis was suggested by Coleman et al. (2005) for the cycles and also was proposed to account for compositional variation in the Tuolumne Intrusive Suite lobes and, by extension, to the Suite as a whole (Economos et al., 2010; Memeti et al., 2010).

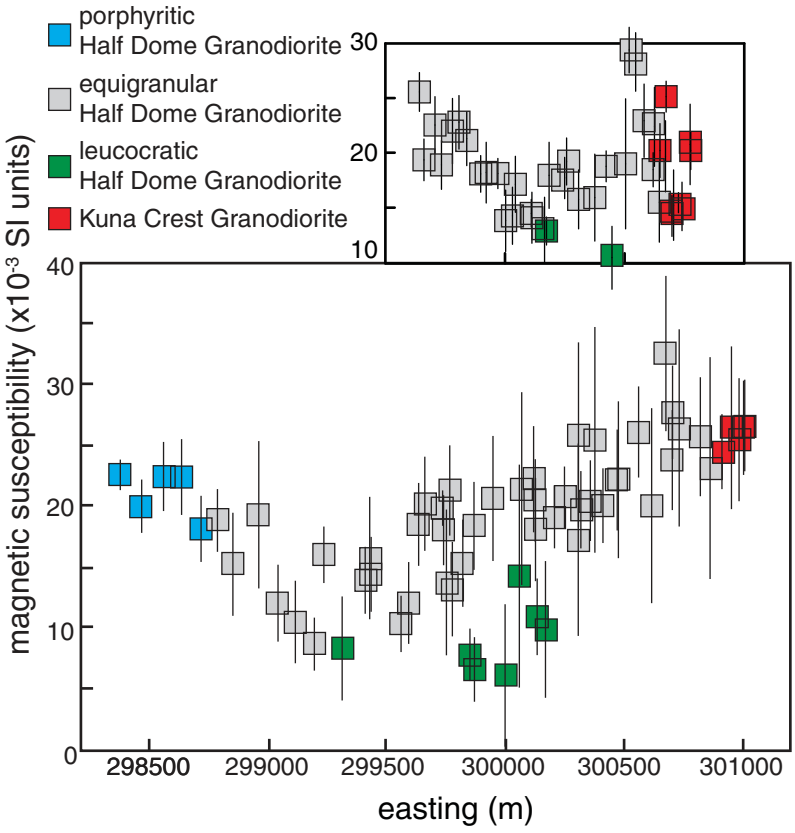

Figure 5. Magnetic susceptibility traverses through the eastern portion of the Half Dome Granodiorite (Khd) (see Fig. 2 for locations of traverses). The distinction between "porphyritic," "equigranular," and "leucocratic" facies is made on the basis of field descriptions of survey sites. The pattern of magnetic susceptibility variation is the mirror image of that mapped on the western side of the granodiorite. On the east, the gradational variation from "normal" to leucocratic Khd occurs from west to east. A sharp contact back to the normal granodiorite occurs on the eastern side of the cycle. In both the east and west sides of the Khd, the best-developed cycle is the innermost (adjacent to the porphyritic facies of the granodiorite).

Aplite Dikes

The major- and trace-element geochemistry of leucocratic Half Dome Granodiorite resembles that of aplites (Figs. 7A and 8A). Although this suggests a common origin, field and petrographic data suggest that the leucocratic phases of the cycles are not late aplite dikes as mapped by Kistler (1973). Whereas injection of a high-silica magma can account for the leucocratic Half Dome Granodiorite, it cannot account for the field relations, the observed cyclicity, or the spatially coherent variation in chemistry with a cycle (Fig. 6). Texturally, leucocratic Half Dome Granodiorite is the same as normal Half Dome Granodiorite, characterized by euhedral hornblende crystals in a matrix of subhedral, medium-grained quartz and feldspar (Figs. 4A and 4B). The texture is not micrographic as is typical of aplites. The hornblende phenocrysts may be entrained crystals from normal Half Dome Granodiorite, but they are conspicuously absent from typical discordant aplite dikes. Only the western (outer) contact of leucocratic rocks in the cycles has a sharp, intrusive relationship with the granodiorite (Figs. 2 and 4C). The eastern contact is consistently gradational in petrography, geochemistry, and magnetic susceptibility (Fig. 6). Thus the leucocratic Half Dome Granodiorite does not appear to have intruded as dikes.

Temporal Variation in Composition of Source Magmas

Zonation in plutonic rocks might reflect variations in the compositions of magmas feeding shallow plutons with little or no differentiation at the level of emplacement (Stevens et al., 2007; Clemens et al., 2010; Tappa et al., 2011). However, for this mechanism to account for the variation preserved in the Half Dome Granodiorite, it would have to operate cyclically. Whereas the Rio Hondo pluton investigated by Tappa et al. (2011) preserves a single monotonic temporal progression from leucogranite to mafic granodiorite, the Half Dome Granodiorite cycles

TABLE 1. MAJOR- AND TRACE-ELEMENT ANALYSES FOR SAMPLES OF SIERRA NEVADA BATHOLIH LEUCOGRANITES AND THE HALF DOME GRANODIORITE CYCLE

Sample	Kjp08-1	Kjp08-4	Kb08-7	Kb08-9	Kb08-10	Krm08-11	Krm08-12	Krm08-13	Kt08-14	Kc08-153
Easting*	291257	292349	373109	372530	372410	374064	374064	374911	377174	374008
Northing	4191117	4191733	4070135	4070314	4070448	4094814	4094814	4094877	4094865	4095749
SiO_2§	75.67	74.30	72.66	75.12	72.24	77.23	73.14	76.65	76.16	75.98
Al_2O_3	13.15	13.47	13.00	12.59	14.30	12.60	13.55	13.52	13.03	13.22
FeO(T)	0.61	1.07	3.41	0.99	1.67	0.19	1.35	0.17	0.74	0.63
MnO	0.04	0.05	0.06	0.05	0.06	0.01	0.05	0.02	0.04	0.09
MgO	0.09	0.15	0.28	0.08	0.32	0.04	0.26	0.05	0.11	0.22
CaO	0.75	1.04	0.70	0.46	0.80	0.39	1.33	1.21	0.58	0.90
Na_2O	3.50	3.34	4.04	3.46	4.56	3.00	3.53	5.97	2.97	3.60
K_2O	5.20	4.99	4.33	5.34	4.64	6.11	4.58	0.79	6.27	4.31
TiO_2	0.09	0.12	0.24	0.15	0.28	0.04	0.18	0.11	0.09	0.16
P_2O_5	0.03	0.03	0.06	0.03	0.08	0.04	0.07	0.02	0.04	0.04
LOI	0.68	0.52	0.58	0.43	0.49	0.41	0.48	0.45	0.42	0.60
Total	99.81	99.06	99.36	98.71	99.44	100.10	98.52	98.96	100.40	99.75
Sc#	3	3	3	1	2	2	3	2	2	4
Be	2	2	2	3	5	1	2	2	1	3
V	B.D.L.**	6	20	5	18	B.D.L.	13	6	B.D.L.	7
Co	B.D.L.	B.D.L.	8	B.D.L.	1	B.D.L.	1	B.D.L.	B.D.L.	B.D.L.
Zn	B.D.L.	B.D.L.	B.D.L.	30	40	B.D.L.	50	B.D.L.	B.D.L.	B.D.L.
Ga	14	17	16	15	17	15	18	15	14	16
Ge	1.8	1.3	1.4	1.3	1.9	2.8	1.4	1.5	2.2	2.2
Rb	197	195	116	159	138	231	200	27	200	203
Sr	92	164	75	43	103	64	225	155	115	155
Y	18.8	11.7	28	19	26.1	34.4	16.7	18.5	25.7	39.6
Zr	58	132	218	139	243	38	121	66	73	105
Nb	16.8	9.7	16.9	20	27.5	27.4	13.5	22.8	9.7	28.9
Cs	2.5	5.9	0.6	2.6	1.5	3.1	5.9	0.3	2.7	2.1
Ba	466	946	389	168	386	195	715	61	545	670
La	28	33.7	36.9	35.8	37.4	17.1	34.8	20	25.6	39.7
Ce	54.8	61.2	76.6	65	86.9	41.7	65.9	39.9	50.4	78.2
Pr	4.99	7.02	8.38	6.71	7.61	5.3	6.3	3.63	4.62	9.17
Nd	18.9	21.2	25.2	19.3	24.4	19	23.2	12.3	17.9	28.4
Sm	3.97	3.48	4.7	3.32	4.41	4.17	4.86	2.61	4.02	5.73
Eu	0.5	0.675	0.553	0.376	0.592	0.269	0.62	0.445	0.534	0.646
Gd	3.79	2.37	3.47	2.34	3.54	3.61	3.28	2.41	2.64	5.4
Tb	0.55	0.33	0.64	0.41	0.63	0.76	0.49	0.46	0.53	0.93
Dy	2.98	1.83	4.19	2.57	4.05	5.3	2.67	3.07	3.75	5.92
Ho	0.58	0.38	0.89	0.55	0.91	1.12	0.49	0.69	0.83	1.3
Er	1.77	1.17	2.85	1.83	3.03	3.26	1.31	2.2	2.53	4.24
Tm	0.283	0.181	0.439	0.316	0.491	0.515	0.201	0.343	0.396	0.649
Yb	1.98	1.19	2.96	2.38	3.45	3.52	1.31	2.2	2.59	4.07
Lu	0.322	0.188	0.437	0.383	0.541	0.57	0.206	0.329	0.408	0.614
Hf	2.3	4.2	6.1	3.9	10.8	3.2	4.3	3.6	3	3.4
Ta	1.67	1.04	1.36	2.19	2.49	2.46	1.22	2.35	1.3	3.24
Tl	1.49	1.15	0.5	0.77	0.57	1.13	1.78	0.12	2.13	1.44
Pb	14	28	8	23	16	20	23	5	23	18
Th	14.4	17.8	10.9	15.1	12.7	10.5	25.6	15.8	18.2	24.5
U	2.94	5.85	2.2	5.5	3.35	10.6	7.22	6.96	4.44	4.59

(*Continued*)

TABLE 1. MAJOR- AND TRACE-ELEMENT ANALYSES FOR SAMPLES OF SIERRA NEVADA BATHOLITH LEUCOGRANITES AND THE HALF DOME GRANODIORITE CYCLE (*Continued*)

Sample	Kc08-155	JBHD07-1	JBHD07-2	JBHD07-3	JBHD07-4	JBHD07-5	JBHD07-6	JBHD07-7	JBHD07-8	JBHD07-9
Easting*	374186	282609	282748	282604	282406	281998	281540	281299	280912	281109
Northing	4095521	4189447	4189612	4189638	4189714	4189880	4189843	4189868	4190306	4190359
M. sus.†		26.97	28.79	31.16	23.09	25.60	28.17	17.64	14.40	7.16
SiO_2§	75.07	65.96	64.50	65.22	66.50	67.03	66.65	71.02	71.14	77.39
Al_2O_3	13.33	16.15	15.96	15.98	14.74	15.37	15.31	14.47	14.17	13.04
FeO(T)	1.00	3.46	3.74	3.82	4.42	3.55	3.19	2.73	1.87	0.56
MnO	0.05	0.07	0.07	0.08	0.11	0.07	0.07	0.07	0.04	0.02
MgO	0.22	1.44	1.53	1.65	1.89	1.48	1.36	1.15	0.69	0.14
CaO	0.96	4.13	4.33	3.92	3.31	3.61	3.56	3.04	2.38	1.44
Na_2O	3.42	3.75	3.85	3.71	3.34	3.32	3.54	3.46	3.23	3.65
K_2O	4.86	3.22	2.76	3.33	3.86	3.78	3.49	3.68	3.83	3.89
TiO_2	0.15	0.58	0.55	0.55	0.64	0.45	0.49	0.42	0.28	0.09
P_2O_5	0.04	0.22	0.23	0.23	0.23	0.20	0.18	0.14	0.11	0.04
LOI	0.52	0.42	0.53	0.74	0.61	0.70	0.38	0.41	0.65	0.24
Total	99.63	99.80	98.48	99.65	100.10	99.97	98.57	100.90	98.58	100.60
Sc#	3	5	5	5	7	6	5	5	2	B.D.L.
Be	2	2	2	2	2	2	2	2	2	3
V	7	79	82	82	89	72	66	55	28	7
Co	B.D.L.	7	8	9	9	7	7	6	3	B.D.L.
Zn	B.D.L.	60	70	70	120	60	60	50	40	B.D.L.
Ga	15	16	18	18	17	15	16	16	15	13
Ge	2.1	1	1	1.1	1.3	1	1	1.2	1	1.2
Rb	222	89	88	115	146	106	110	129	131	178
Sr	160	653	658	633	417	545	493	395	410	147
Y	23.3	9.1	8.8	7.7	10.1	8.1	11	8.5	8.3	2
Zr	80	118	132	125	139	114	123	95	83	39
Nb	17.9	6.5	6.4	5.4	8.2	5.6	8.5	7.9	7.7	3.1
Cs	3.9	4.2	3.6	5.6	7	5.6	5.7	6.4	4.1	34.3
Ba	879	1066	845	982	703	1049	783	624	821	115
La	29.3	25.3	26.2	25.8	33.7	32.5	23.9	19.9	25.9	12
Ce	62.9	49.2	49.3	44.5	58.8	51.2	53.2	43.5	48.5	16.3
Pr	5.65	5.38	5.05	4.65	5.84	4.72	5.78	4.8	4.9	1.25
Nd	19.3	19	17.8	16.2	20	15.5	20	16.3	16.1	3.42
Sm	3.98	3.21	3.08	2.71	3.39	2.52	3.38	2.71	2.53	0.51
Eu	0.657	0.967	0.953	0.886	0.852	0.794	0.974	0.766	0.707	0.189
Gd	3.52	2.61	2.58	2.31	2.87	2.22	2.99	2.38	2.03	0.42
Tb	0.61	0.35	0.34	0.3	0.37	0.3	0.4	0.32	0.28	0.05
Dy	3.89	1.71	1.71	1.49	1.93	1.53	2.09	1.65	1.42	0.3
Ho	0.85	0.31	0.29	0.27	0.34	0.27	0.38	0.3	0.27	0.06
Er	2.63	0.86	0.83	0.76	1.01	0.78	1.1	0.91	0.8	0.21
Tm	0.408	0.126	0.119	0.111	0.154	0.118	0.173	0.136	0.125	0.038
Yb	2.65	0.82	0.8	0.72	1.01	0.83	1.18	0.94	0.85	0.3
Lu	0.398	0.128	0.129	0.113	0.16	0.132	0.181	0.157	0.134	0.064
Hf	3.5	3.4	3.7	3.6	4.3	3.3	3.9	3.4	2.8	2
Ta	1.23	0.64	0.59	0.54	0.89	0.64	1.2	1.12	1.1	0.32
Tl	1.19	0.53	0.34	0.56	0.75	0.52	0.52	0.59	0.57	0.79
Pb	30	27	43	27	30	37	69	38	43	46
Th	14.4	16.7	9.6	8.41	23.5	17.1	19.4	25.7	19	17.5
U	2.06	11.9	3.91	4.92	6.11	5.85	8.8	12.8	6.28	12.6

(*Continued*)

TABLE 1. MAJOR- AND TRACE-ELEMENT ANALYSES FOR SAMPLES OF SIERRA NEVADA BATHOLITH LEUCOGRANITES AND THE HALF DOME GRANODIORITE CYCLE (*Continued*)

Sample	JBHD07-10	YO-23	YO-24	YO-25	YO-26	YO-27	YO-28
Easting*	281235	282838	282750	282714	282570	282469	282432
Northing	4190337	4190513	4190479	4190472	4190066	4189942	4189432
M. sus.†	18.03	19.51	19.40	18.37	14.58	10.66	6.33
SiO_2§	69.16	66.39	63.76	63.41	70.27	73.20	75.23
Al_2O_3	15.52	16.94	16.91	15.83	14.55	13.97	13.50
FeO(T)	2.49	2.73	4.26	4.42	2.61	1.70	1.20
MnO	0.06	0.06	0.09	0.10	0.07	0.05	0.04
MgO	1.07	1.32	2.06	1.90	0.97	0.53	0.31
CaO	3.12	3.91	4.31	4.25	2.79	2.20	1.53
Na_2O	3.59	3.82	3.78	3.74	3.60	3.34	3.46
K_2O	3.51	3.76	3.45	3.28	3.61	4.10	4.55
TiO_2	0.38	0.43	0.59	0.62	0.39	0.24	0.14
P_2O_5	0.13	0.15	0.21	0.22	0.14	0.11	0.06
LOI***	0.66	0.48	0.45	0.29	0.31	0.55	0.25
Total	99.97	100.30	100.30	98.54	99.58	100.20	100.40
Sc#	4	4	7	8	4	2	2
Be	2	2	2	2	2	2	2
V	49	56	87	90	49	32	18
Co	5	8	11	10	5	3	2
Zn	90	50	80	70	50	30	30
Ga	17	19	21	20	18	16	17
Ge	1.2	1.1	1.3	1.3	1.4	1.3	1.6
Rb	117	111	133	122	138	146	197
Sr	472	688	641	567	389	320	202
Y	9.3	8.5	10.3	15.1	9.4	6.1	2.8
Zr	93	88	115	131	107	92	61
Nb	7.5	4.9	6.3	8.2	7.4	5.7	4.6
Cs	7.1	3.4	6	5.3	5.6	4.1	6.2
Ba	1082	1487	1221	995	600	592	259
La	25.1	19.3	23.8	27.7	28.7	29.3	16.6
Ce	49.1	38.3	47.9	61.5	50.6	44.8	21.6
Pr	5.11	4.04	5.05	6.9	4.82	3.76	1.65
Nd	16.8	15	18.3	26.5	16.5	12.1	5.07
Sm	2.82	2.45	2.86	4.47	2.76	1.79	0.76
Eu	0.844	0.776	0.941	1.17	0.729	0.534	0.242
Gd	2.38	1.83	2.21	3.41	1.95	1.26	0.5
Tb	0.33	0.28	0.32	0.52	0.3	0.19	0.08
Dy	1.74	1.48	1.7	2.72	1.62	1.03	0.43
Ho	0.32	0.27	0.32	0.49	0.3	0.19	0.09
Er	0.95	0.76	0.91	1.38	0.85	0.57	0.27
Tm	0.148	0.113	0.142	0.207	0.126	0.09	0.044
Yb	0.97	0.73	0.96	1.34	0.83	0.63	0.33
Lu	0.147	0.11	0.144	0.197	0.141	0.102	0.061
Hf	2.9	2.5	3.3	3.9	3.6	3	2.8
Ta	0.97	0.6	0.8	1.14	0.88	0.68	0.43
Tl	0.59	1.21	0.67	0.7	0.7	0.64	0.89
Pb	78	17	15	18	22	23	28
Th	18.9	6.52	23.7	86.6	27.4	32.3	26.4
U	5.69	2.27	4.66	12.1	8.13	23.2	5.43

*All coordinates NAD 83, section 11S.
†Magnetic susceptibility (M. sus.) reported as the average. Full data set in Supplemental Table 1 (see footnote 1).
§All oxides reported as weight percent.
#All trace elements reported as ppm.
**Below detection limit (B.D.L.); ***Loss on ignition.

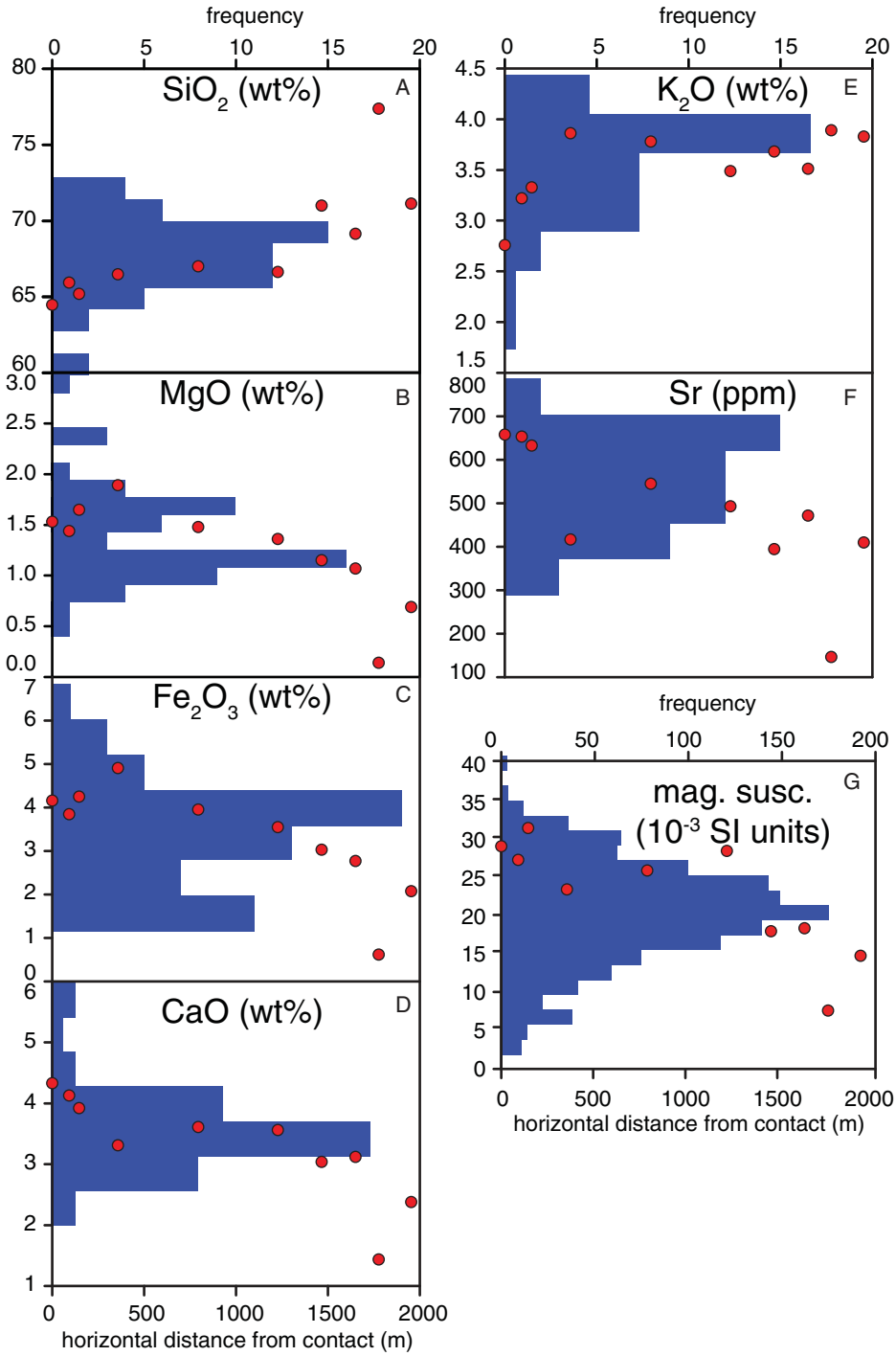

Figure 6. Histograms of compositional data from the Half Dome Granodiorite (Khd) (Bateman et al., 1984; Gray et al., 2008) plotted with spatial variation in composition within an individual cycle (red symbols). Histogram bin size is selected to give 15–20 analyses in the largest bin. The cycle shows a consistent variation toward higher SiO_2 and K_2O, and lower MgO, Fe_2O_3, CaO, Sr, and magnetic susceptibility toward the west. The data for the cycle span and slightly exceed the range of compositions reported from across the Khd, but are centered on the mode for the regional data set. This suggests that the variation preserved in the cycle reflects internal differentiation of the "normal" Khd into a mafic (eastern) base and a silicic (western) top.

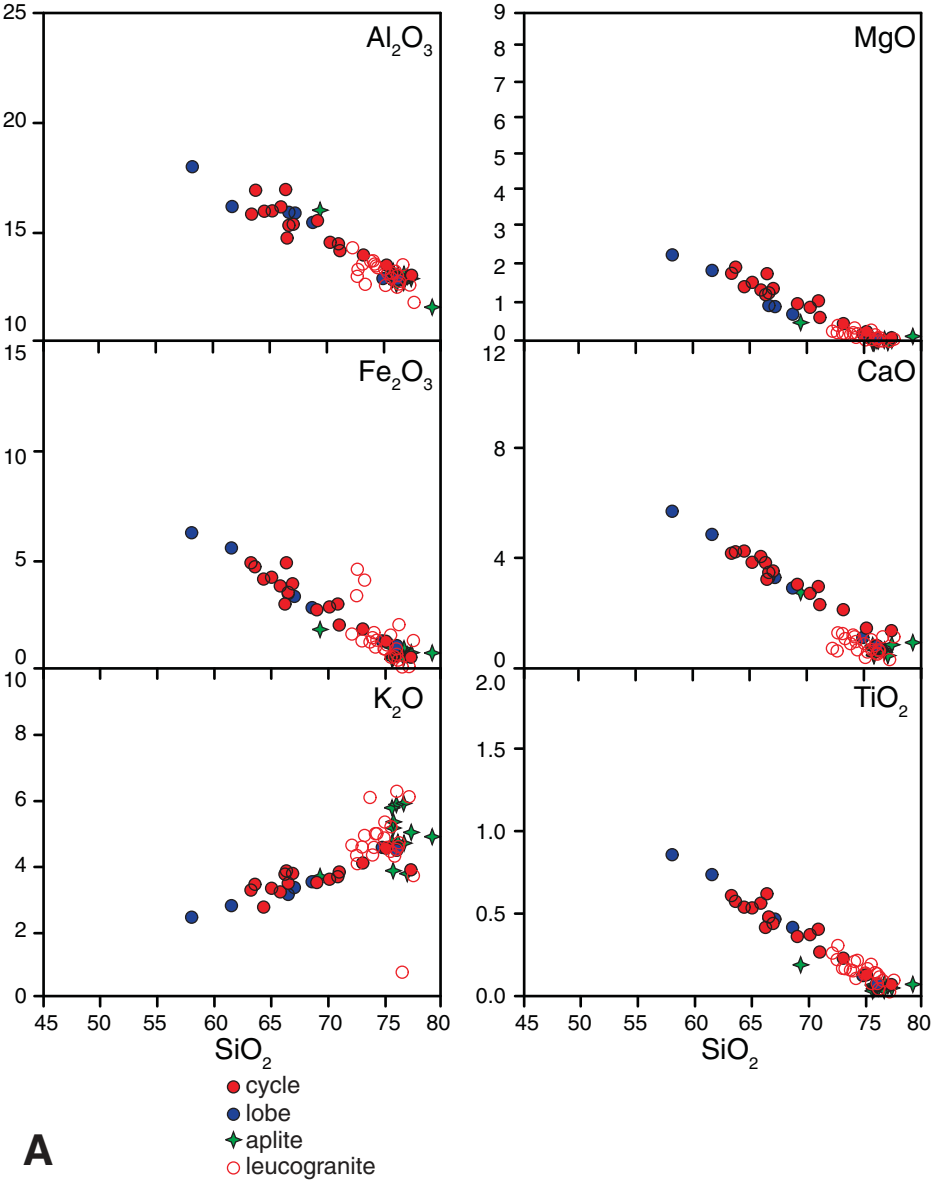

Figure 7 (*Continued on following pages*). Major-element variation Harker diagrams for the rocks in the Half Dome Granodiorite (Khd) (Bateman et al., 1984; Gray et al., 2008), Sierra Nevada batholith (Frost and Mahood, 1987; Wenner and Coleman, 2004), Sierran aplites (Glazner et al., 2008), Sierran leucogranites (Wenner and Coleman, 2004; this study), Sierran metavolcanic rocks (Sorensen et al., 1998; Barth et al., 2011), Khd lobe (Economos et al., 2010), and the Khd cycle (this study). All data are plotted as weight % oxide. (A) Data for cycles, the lobe, leucogranites, and aplites. High-silica samples from the cycles and lobe are similar to leucogranites and aplites.

preserve at least seven such compositional shifts (Fig. 2). If the regional pattern of younging toward the center of the Tuolumne Intrusive Suite is mimicked at the scale of the cycles, the progression from leucocratic Half Dome Granodiorite to mafic Half Dome Granodiorite from west to east might be similar to that observed in the Rio Hondo pluton. According to this interpretation, each cyclic variation in petrography reflects a spatial progression in which the magma was being intruded coupled with a gradational change from high-silica magma toward low-silica magma, with compositional variability derived from the source. The sharp contact at the east side of a cycle might represent a brief hiatus in intrusion that is also marked by a return to intrusion of high-silica magma.

Although this interpretation is difficult to test, it seems unlikely because the repeated pattern of evolution from leucocratic to mafic Half Dome Granodiorite, and apparent temporal progression from low-volume, poorly developed cyclic variation (thin outer cycles) to high-volume, well-developed variation (thick inner cycles), is difficult to reconcile with a melt generation model. If variable entrainment of peritectic crystals derived during melting drives the chemical variation in the cycle (Stevens et al., 2007; Clemens et al., 2010), the variation in crystal load would have to be very consistent within a cycle, and repetitious in order to generate multiple cycles. In addition, trace-element variation with major oxides within cycles (and lobes) is very consistent (Fig. 8A) and does not show the scatter that might be attributed to variations in the composition of the source, or variations in the entrainment of accessory phases (Villaros et al., 2009).

In Situ Crystal/Liquid Separation

The similarity between the major- and trace-compositions of leucocratic Half Dome Granodiorite and aplites is consistent with a similar origin for both. Aplites are generally accepted to be the products of shallow-crustal crystal/liquid separation (Eichelberger et al., 2006; Glazner et al., 2008), and we propose the same origin for the leucocratic Half Dome Granodiorite. However, rather than intruding as dikes, the leucocratic Half Dome Granodiorite appears to have collected at the western margins of the cycles.

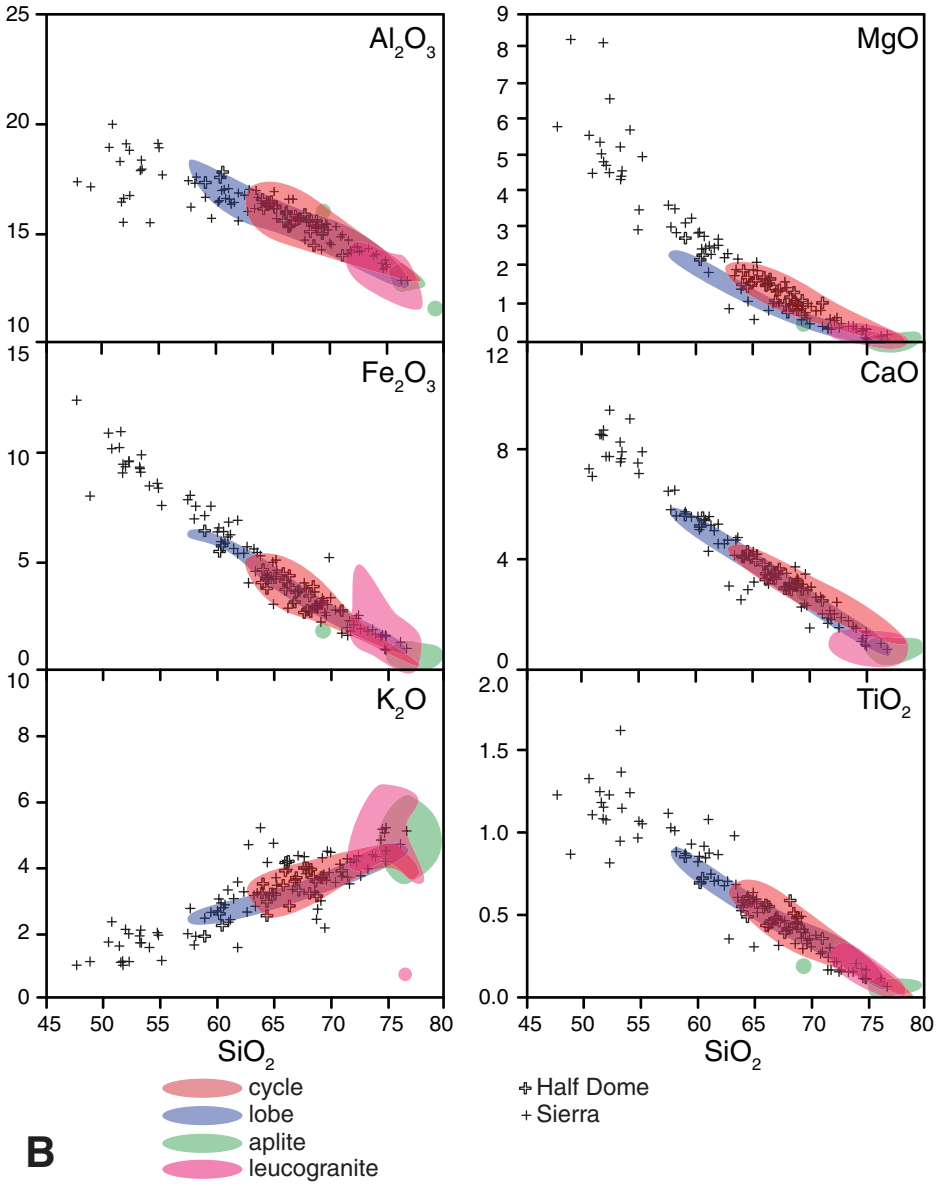

Figure 7 (*Continued*). (B) Samples from (A) are simplified as fields. Data for the Khd and other plutonic rocks from the Sierra Nevada batholith are added. The cycle and lobe data span the range of compositions previously reported for the Khd. The samples from the batholith extend the range of compositions to lower SiO_2, but otherwise overlap with the other data sets.

The steep westward dips of cycle contacts and the local intrusion of leucocratic Half Dome Granodiorite into adjacent cycles are consistent with the accumulation of high-silica magma against the roof of the evolving magma chamber (Fig. 10). According to this interpretation, chemical variation in the normal Half Dome Granodiorite reflects variable loss of late high-silica liquid to the high-silica portion of the cycle. This interpretation is supported by the regular spatial variation in the chemistry of the cycle from east (mafic) to west (felsic; Fig. 6).

The geochemical variation of the analyzed cycle mimics that of the lobes (Economos et al., 2010; Memeti et al., 2010). These authors interpreted the geochemical variation in the lobes to be the result from in situ crystal/liquid separation (Figs. 7A and 8A). Compared to aplite dikes, however, leucocratic Half Dome Granodiorite at the top of cycles and within lobes reflects less complete separation of the melt from a hornblende-bearing crystal residue and a shorter transport distance; that is, cycle-tops remained with the partial-melt zones from which they were derived, whereas aplite dikes represent the same melt intruded outward into country rock.

Model for the Origin of the Half Dome Cycles

We suggest that each cycle represents a zone of mush that separated into a lower (eastern) melt-depleted base grading upward to a melt-rich top (Fig. 10). If the cycles share a common origin with the lobes in the Tuolumne Intrusive Suite, geochronologic data suggest that they were assembled incrementally over hundreds of thousands of years (Memeti et al., 2010). Geochronologic data for rocks in the area of the mapped cycles indicate that accumulation of the magmas occurred over 1.5–2.0 Ma (Coleman et al., 2004; Memeti et al., 2010). Thus, whereas magmas forming a single cycle may accumulate on the order of 10^5 years, the repetitious process of intrusion and evolution in Half Dome Granodiorite is cyclic on the order of 10^6 years. The model proposed here closely follows new ideas regarding the nature and evolution of complex, incrementally assembled magma systems (e.g., Walker et al., 2007; Miller et al., 2011).

We propose that cycles (and lobes) were intruded incrementally as pulses of

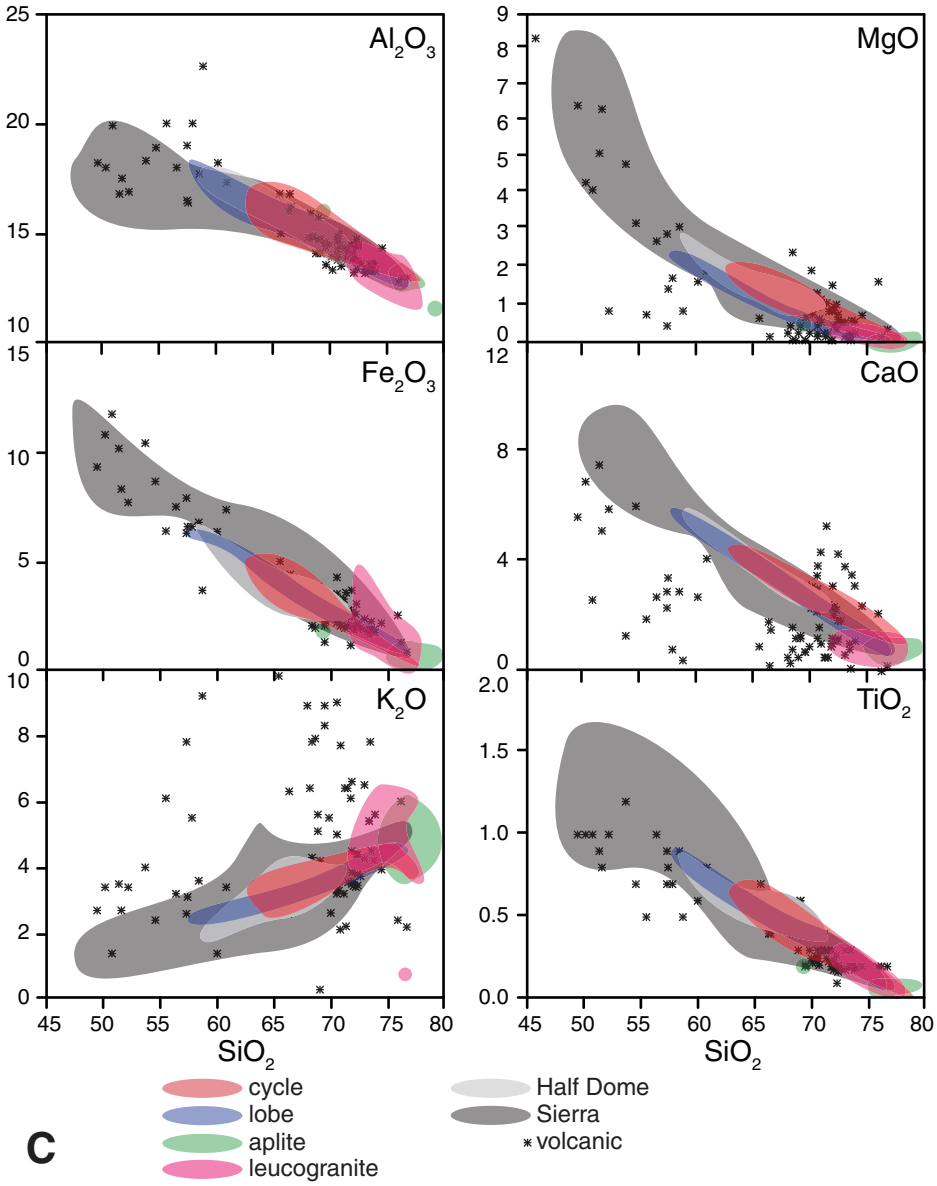

Figure 7 (*Continued*). (C) All the data fields in comparison to data for metavolcanic rocks from the Sierran arc. Deviation in the metavolcanic rocks is typical of alkali element metasomatism (Sorensen et al., 1998; Barth et al., 2011). See text for discussion.

crystal-poor melts. During crystallization the cycles were periodically refreshed by heat and fluids derived from underplated melt that increased the fraction of silicic melt in mush. The sharp upper contacts of the cycles may have formed when the heat flux into the growing pluton dropped below that required to maintain interstitial melt, and thus the cycle solidified completely. A subsequent increase in magma flux then initiated a new, structurally deeper cycle. The gradual disappearance of cyclic compositional variations inward from both the east and the west suggests that, late in the assembly of the Tuolumne Intrusive Suite, sufficient thermal inertia accumulated that pore melt was continuously present as the pluton grew, although this is difficult to test.

The formation of cycles only along the outer (older) margins of the Half Dome pluton indicates that they developed only during the early intrusive history of the Tuolumne Intrusive Suite. Thermal models of incremental pluton growth predictably show an evolution from initial pulses that quickly drop below the solidus to pulses that remain at super-solidus temperatures for geologically significant time periods and, depending on the intrusion rate, do not drop below the solidus temperature before the next pulse intrudes (e.g., Hanson and Glazner, 1995). The progression of the cycles from thin and poorly developed on the older, outer margins of Half Dome Granodiorite to the thickest, well-defined cycle in the younger, interior portion of the pluton is consistent with this interpretation (Fig. 10). Depending on the geometric arrangement of successive pulses, it is possible to evolve to a system in which the partial-melt zone does not match either the size or the shape of the increments from which it is constructed (Bartley et al., 2007).

The Origin of Leucogranites

The contrast between the trace-element geochemistry of isolated leucogranite plutons, and the leucocratic Half Dome Granodiorite and aplites indicates that they cannot share a similar origin (Fig. 8A). Glazner et al. (2008) attributed the depletion of the HFSEs and MREEs in aplites to separation of the aplite liquids from titanite-bearing crystal mush, which is also

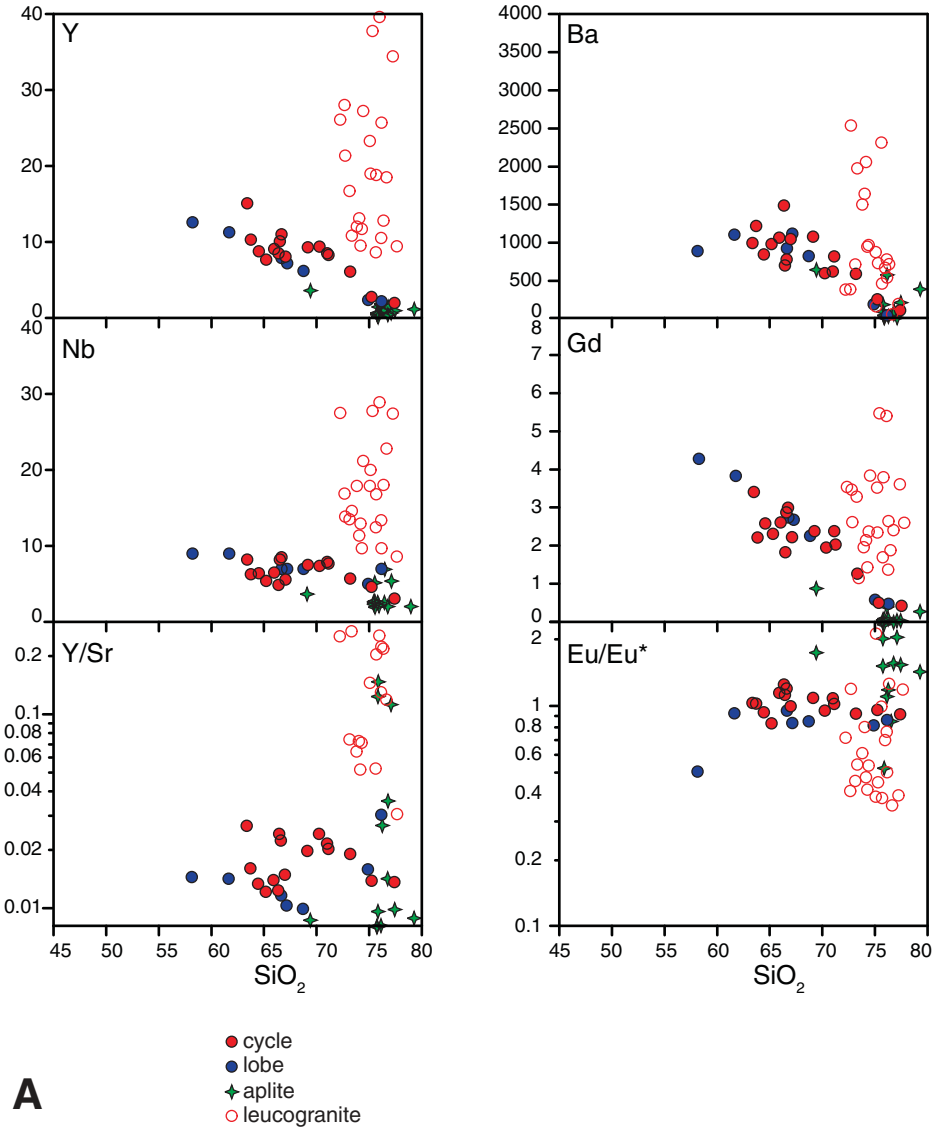

Figure 8 (*Continued on following pages*). Trace-element variation Harker diagrams for the rocks in this study. Data sources and symbols are the same as in Figure 7. SiO_2 plotted as weight % oxide. Trace-elements plotted as ppm. (A) Data for cycles and lobes deviate significantly away from the compositions of leucogranites at high SiO_2, but they consistently plot with aplites. Notably, the cycle and lobe trend toward significant middle rare earth element (MREE) depletion (shown here as [Gd]), Y, and high field strength elements (HFSEs) (Nb) that is typical for titanite removal.

consistent with the proposed origin of cycles and lobes (Fig. 8A). This suggests that magmas that formed the isolated leucogranite plutons of the Sierra Nevada evolved in the absence of titanite. We envision two alternative hypotheses to account for this observation: either the leucogranites evolved through shallow-crustal crystal/liquid separation in titanite-free magmas, or they did not inherit their chemical signature in the shallow crust, but instead carried a melting signature from deeper in the crust.

Crystal/Liquid Separation in the Absence of Titanite

It is possible that leucogranites lack a titanite removal signature, yet still formed by crystal/liquid separation in a shallow-crustal reservoir, because they formed as hot-reduced melts (Bachmann and Bergantz, 2008), or because titanite joined the crystallizing mineral assemblage late in the sequence. Stability of titanite is controlled in part by oxygen fugacity, and lower crystallization temperatures are promoted by lower oxygen fugacity (Lipman 1971; Wones, 1989). Because exposed eastern Sierra granodiorites are ubiquitously high–f_{O_2} magnetite-series rocks (Ague and Brimhall, 1988), the possibility that the leucogranites were derived from reduced melts seems unlikely.

Alternatively, if titanite is a late crystallizing phase in the granodiorites, separation of leucogranites from associated crystal mushes relatively early in the crystallization history of a mush could explain the lack of the titanite removal signature in their chemistry (Columbini et al., 2011). According to this hypothesis, separation of low-volume aplites, and magmas forming the leucocratic portions of cycles and lobes, occurs relatively late in the history, after titanite has started to crystallize.

It is difficult to fully evaluate this hypothesis in the light of existing data. The general scarcity of titanite in volcanic rocks (Nakada, 1991) argues for introduction of titanite into typical crystallizing assemblages after several tens of percent crystallization. An argument against late crystallization of titanite is that it generally forms euhedral crystals up to 1 cm across in plutonic rocks. However, the large euhedral character of K-feldspar megacrysts is often interpreted to be the result of textural coarsening after a rock is largely crystallized (Higgins, 2000), perhaps driven by thermal cycling (Johnson and Glazner, 2010). Crystallization of titanite under the same conditions, or in melt pockets larger than the titanite crystals, may favor growth of euhedral crystals as well.

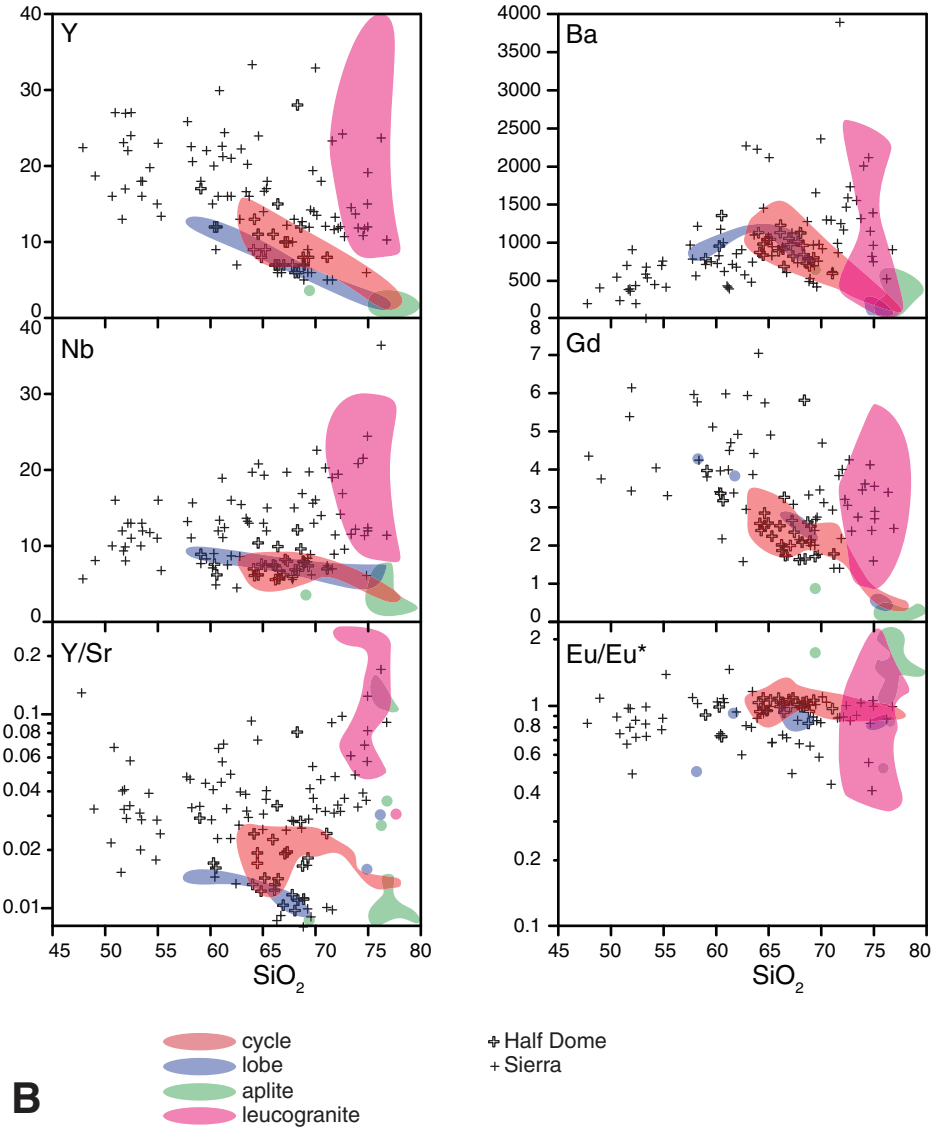

Figure 8 (*Continued*). (B) Trace-element data for the Half Dome Granodiorite (Khd) and Sierra Nevada batholith have significant scatter, but do not reach the extremes in composition defined by aplites.

A final argument against late titanite crystallization to account for the geochemistry of Sierra Nevada batholith leucogranites is that the mineral assemblage of the Fish Canyon Tuff is the same as a typical Sierran granodiorite, including the occurrence of titanite, yet it is also only ~45% crystalline (Bachmann et al., 2005). Furthermore, the glass (liquid) in the tuff is a high-silica rhyolite that shows geochemical evidence of titanite removal comparable to that of aplites (Glazner et al., 2008). This shows that titanite can be present at fairly high melt fraction in an intermediate magma.

Origin of Leucogranites as Deep-Crustal Melts

The similarity of radiogenic-isotope geochemistry of coeval diorites and granites in the central Sierra Nevada batholith led to the suggestion that the felsic rocks may be derived by partial melting of coeval mafic rocks (Coleman et al., 1992; Wenner and Coleman, 2004). Subsequent experimental work demonstrates that high-silica liquids similar in composition to exposed Sierran granites can be generated by partial melting at mid- to lower-crustal pressures of hydrous, potassic mafic rocks similar to the sparse mafic rocks exposed in the batholith (Sisson et al., 2005). Trace-element modeling of the same experimental run products by Ratajeski et al. (2005) suggests that the trace-element geochemistry of the high-silica melts might also be a good match for the granite. These observations are consistent with the possibility that the isolated leucogranites represent primary deep-crustal melts.

According to this hypothesis, the dominant geochemical signal in the Sierra Nevada batholith as a whole is governed by melting processes at the source. Leucogranites represent one end member, a low melt-fraction composition that is generated during partial melting in the deep crust (Figs. 7B and 8B). The rare earth element (REE) patterns and trace-element geochemistry (e.g., Sr and Eu depletion, HFSE, and Y enrichment) therefore reflect deep melting rather than shallow-crustal crystal/liquid separation (Hildreth, 2004). The relative scarcity of leucogranites exposed in the batholith may be a consequence of the difficulty to amalgamate and move small volumes of high-viscosity melt.

Shallow-crustal crystal/liquid separation is inefficient, and in some places is demonstrably insignificant in generating the compositional variation of shallow plutonic rocks (Clemens et al., 2010; Tappa et al., 2011). A reasonable alternative working hypothesis is that in some

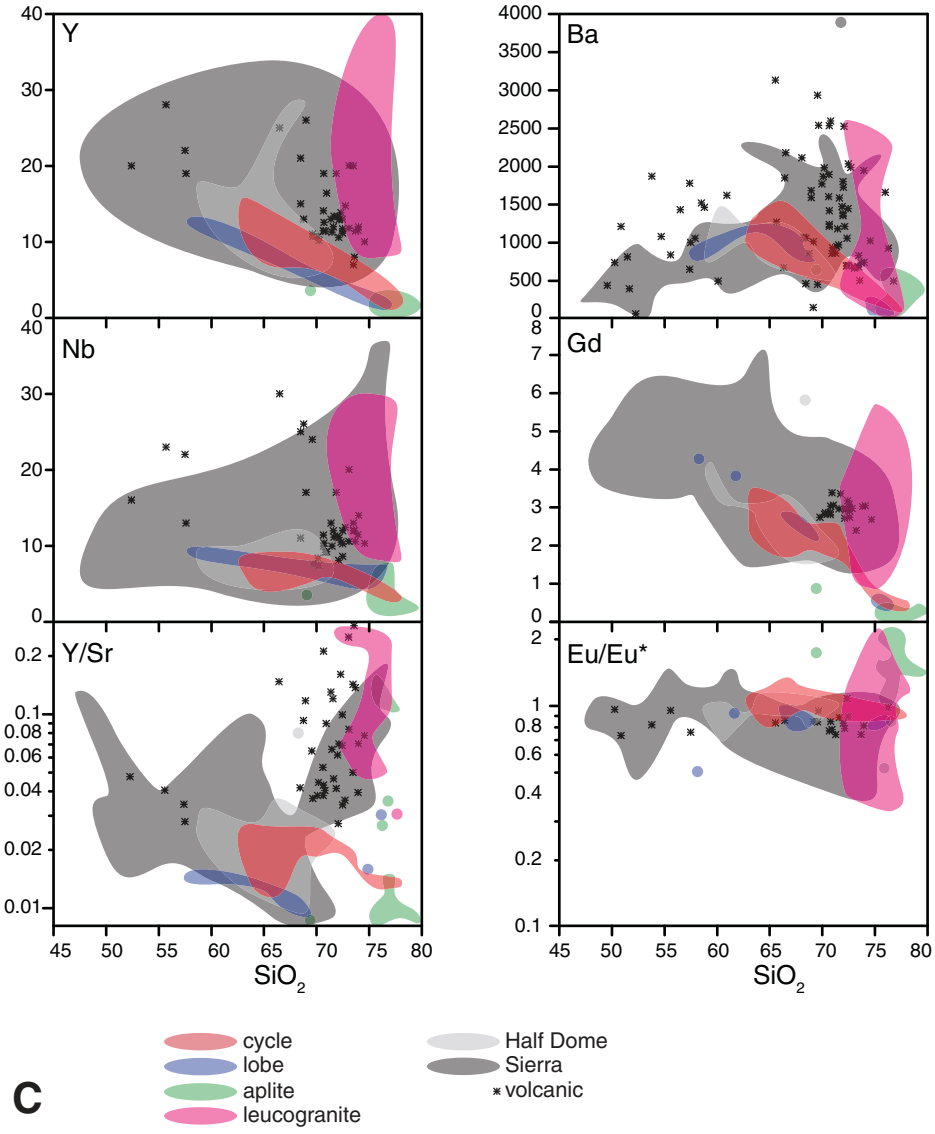

Figure 8 (*Continued*). (C) Metavolcanic rocks track the variation recorded by plutons and leucogranites and deviate substantially from aplites and high-silica members of the cycle and lobe. See text for discussion.

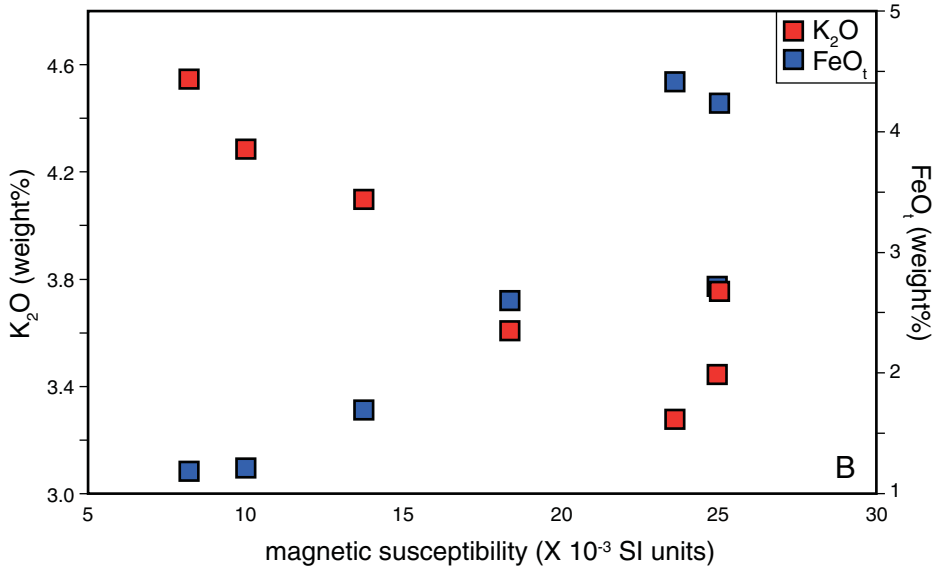

Figure 9. Correlation of chemical and magnetic susceptibility data from a single cycle. The excellent correlations (positive for FeO_{Total}, negative for K_2O) of chemical data with magnetic susceptibility supports the idea that, in fresh, glaciated exposures, magnetic susceptibility measurements provide a fast technique for quantifying chemical variation in the field.

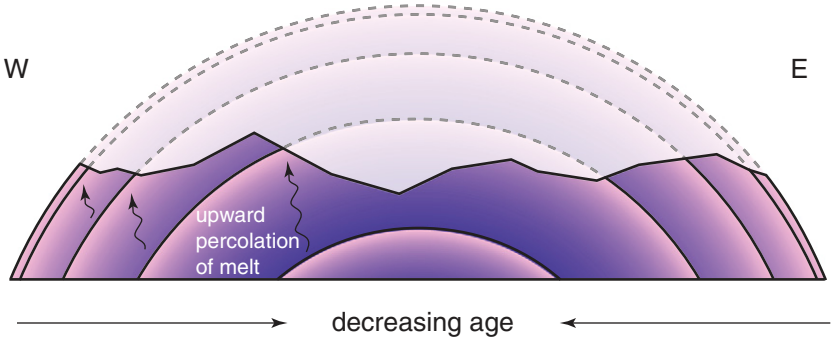

Figure 10. Highly schematic representation of proposed model for the origin of cyclic variations in the Half Dome Granodiorite (Khd). No vertical or horizontal scale is implied. Each cycle is interpreted to represent a zone of interconnected melt during incremental assembly of the granodiorite. The regional age pattern of the Tuolumne Intrusive Suite indicates that units become younger toward the center of the suite (Coleman et al., 2004; Memeti et al., 2010). The mirror-image pattern of cyclic variability and the outward dips from west to east suggests that the cycles may be separated halves of a once continuous laccolithic body. The progressive increase in cycle thickness with decreasing age is interpreted to result from progressive elevation of the geothermal gradient through time (in response to magma accumulation), thus allowing for thicker lenses of interconnected melt. Note, however, that the maximum thickness of the interconnected melt zone need never have exceeded the width of the thickest cycle (~2 km). The top of each cycle is defined by a sharp contact with the base of the previous cycle. We interpret the origin of the distinct cycle base to indicate that enough time passed for the older cycle to completely crystallize before intrusion of a new magma increment initiated formation of the next cycle.

leucogranites, these variations are a source signal. This hypothesis should be tested through experimentation, examination of the chemistry of deep-crustal migmatites where it can be demonstrated that leucosomes formed from melt, and the geochemistry of lower-crustal xenoliths. For example, the hypothesis predicts that the negative Eu anomalies that characterize leucogranites should be balanced by lower-crustal rocks with positive Eu anomalies. At least locally, this may be true (Chen and Arculus, 1995).

Insights into Plutonic/Volcanic Rock Connections

The interpretation presented of the cycles as zones of melt migration during assembly of the Tuolumne Intrusive Suite, with high-silica caps over a crystal-rich mush (Fig. 10), resembles many authors' interpretations of the nature of magma chambers (e.g., Hildreth, 1981, 2004; Lipman, 2007). In sharp contrast, however, we propose that the active zone of crystal/liquid separation was limited to thin cycles, and never approached the volume of the entire intrusive suite (e.g., Walker et al., 2007; Miller et al. 2011). This is consistent with thermal modeling that indicates that plutons such as Half Dome Granodiorite that accumulated at rates on the order of 10^{-3}–10^{-4} km^3a^{-1} (including Half Dome Granodiorite) are assembled far too slowly to support eruptions of 100s of km^3 of magma (Annen, 2009).

More generally, however, if we can distinguish the geochemical signal of source composition variation (regional variation in granodiorites and leucogranites) from shallow-crustal differentiation (variation within cycles and lobes), then we can evaluate the roles of these processes in generating the volcanic rocks produced by the Sierran arc (Sorensen et al., 1998; Barth et al., 2011). Major-element data for the volcanic rocks show evidence for alteration by metasomatism and metamorphism that is particularly evident for K_2O and CaO (Fig. 7C). However, the trace-element data are interpreted to be reliable (Sorensen et al., 1998; Barth et al., 2011), and we restrict our discussion to HFSEs and REEs that should be particularly insensitive to alteration.

The geochemical trends that characterize the Mesozoic volcanic rocks follow the trends defined by intermediate plutonic rocks (Figs. 7C and 8C). At high silica (>72% SiO_2), the chemistry of both volcanic and plutonic rocks diverges sharply from the linear trend defined by lower silica rocks. Thus, high-silica volcanic rocks and leucogranites are geochemically similar, and both are quite distinct from aplites and the leucocratic facies in the Half Dome Granodiorite (Figs. 7C and 8C). This suggests that the processes that generated the range-scale geochemical variation are the same processes that generated the regional variation in the chemistry of the volcanic rocks. These processes appear to be independent of the shallow-crustal crystal/liquid fractionation that generated aplites and the geochemical trends defined by cycles and lobes. Consequently, we conclude that the geochemical trends at the scale of intrusive suites, the batholith and the associated volcanic rocks were governed by melting processes at the source. Shallow-crustal crystal/liquid separation also occurred but it appears to have generated only second-order variations on the main source-derived signal.

In this interpretation, plutonic rocks do not represent residues of crystal/liquid separation that yielded high-silica volcanic rocks (Smith, 1979; Hildreth, 1981, 2004; Bachmann and Bergantz, 2004). Instead, plutonic rocks are coarsely crystalline samples of the same magmas that were erupted from volcanoes (Tappa et al., 2011). Although we suggest that shallow crystal-liquid separation does not appear to be significant in the Sierra Nevada batholith, this need not be true everywhere. If our conclusions are more generally applicable, one of the most important implications is that the plutonic rock record preserves the same information regarding crustal evolution that is inferred for the volcanic rock record. Thus, because plutonic rocks are much more widely preserved than volcanic rocks in the Sierra Nevada batholith (Bateman, 1992) and elsewhere (Mills et al., 2008), there may be a significantly more voluminous record of crustal evolution available for examination than previously appreciated.

CONCLUSIONS

Geochemical data from rocks of the Sierra Nevada batholith define two distinct trends that reflect different processes that appear to have operated at different spatial and temporal scales. We hypothesize that batholith-scale trends reflect extraction of partial melt from the source, and that the repetitious petrographic and geochemical variation that characterizes the cycles and lobes preserved in the Half Dome Granodiorite results from low-pressure crystal/liquid separation. We interpret the source signal to dominate at the regional scale and to govern the geochemical trends of both individual intrusive suites and the batholith as a whole. The crystal/liquid separation trend is expressed at

the kilometer scale within some plutons. Geochemical evidence for pluton-scale, shallow-crustal crystal/liquid separation is conspicuously absent from existing data from the Sierra Nevada batholith. Geochemical variations in the batholith closely resemble those of the associated arc volcanic rocks, indicating that both are end products of the same processes rather than being complementary. Although shallow fractionation is often invoked in linking the plutonic and volcanic rock records, it appears to be of limited importance in the plutons because it would drive melt compositions away from the compositions of erupted magmas. We therefore infer that large-scale geochemical variation is determined primarily at the lower-crustal source of both volcanic and plutonic magmas. We propose that emplacement-level processes such as fractional crystallization produce noise that modifies the main source signal seen in both plutonic and volcanic rocks of the Sierran arc.

ACKNOWLEDGMENTS

This research was supported by National Science Foundation grants EAR-0336070 and EAR-0538129 (Coleman and Glazner), and EAR-0337351 and EAR-0538094 (Bartley). Sam Coleman, Jesse Davis, Breck Johnson, Bryan Law, Ryan Mills, Kent Ratajeski, and Tristan Vrolijk participated in field work and made important contributions to the ideas in this manuscript. We gratefully acknowledge generous cooperation and logistical support from the U.S. National Park Service and U.S. Geological Survey, in particular Jan van Wagtendonk, Peggy Moore, and Greg Stock. We also thank the staff of the White Mountain Research Station for their generous assistance during our work. The manuscript was improved significantly in response to reviews by Calvin Miller and Gary Stevens, and comments from Associate Editor Lang Farmer.

REFERENCES CITED

Ague, J.J., and Brimhall, G.H., 1988, Regional variations in bulk chemistry, mineralogy, and the compositions of mafic and accessory minerals in the batholiths of California: Geological Society of America Bulletin, v. 100, p. 912–927, doi:10.1130/0016-7606(1988)100<0912:MAAADO>2.3.CO;2.

Annen, C., 2009, From plutons to magma chambers: Thermal constraints on the accumulation of eruptible silicic magma in the upper crust: Earth and Planetary Science Letters, v. 284, p. 409–416, doi:10.1016/j.epsl.2009.05.006.

Bachmann, O., and Bergantz, G.W., 2004, On the origin of crystal-poor rhyolites: Extracted from batholithic crystal mushes: Journal of Petrology, v. 45, p. 1565–1582, doi:10.1093/petrology/egh019.

Bachmann, O., and Bergantz, G.W., 2008, Rhyolites and their source mushes across tectonic settings: Journal of Petrology, v. 49, p. 2277–2285, doi:10.1093/petrology/egn068.

Bachmann, O., Dungan, M.A., and Bussy, F., 2005, Insights into shallow magmatic processes in large silicic magma bodies: The trace element record in the Fish Canyon magma body, Colorado: Contributions to Mineralogy and Petrology, v. 149, p. 338–349, doi:10.1007/s00410-005-0653-z.

Baker, B.H., and McBirney, A.R., 1985, Liquid fractionation. Part III: Geochemistry of zoned magmas and the compositional effects of liquid fractionation: Journal of Volcanology and Geothermal Research, v. 24, p. 55–81, doi:10.1016/0377-0273(85)90028-9.

Barth, A.P., Walker, J.D., Wooden, J.L., Riggs, N.R., and Schweickert, R.A., 2011, Birth of the Sierra Nevada magmatic arc; Early Mesozoic plutonism and volcanism in the east-central Sierra Nevada of California: Geosphere, v. 7, p. 877–897, doi:10.1130/GES00661.1.

Bartley, J.M., Glazner, A.F., Coleman, D.S., Kylander-Clark, A.R.C., Mapes, R., and Friedrich, A.M., 2007, Large dextral offset across Owens Valley, California, and its possible relation to tectonic unroofing of the southern Sierra Nevada: Geological Society of America. Special Paper, v. 434, p. 129–148.

Bartley, J.M., Glazner, A.F., and Mahan, K.H., 2012, Formation of pluton roofs, floors, and walls by crack opening at Split Mountain, Sierra Nevada, California: Geosphere, v. 8, p. 1086–1103, doi:10.1130/GES00722.1.

Bateman, P.C., 1992, Plutonism in the central part of the Sierra Nevada Batholith, California: United States Geological Survey Professional Paper, v. 1483, 186 p.

Bateman, P.C., and Chappell, B.W., 1979, Crystallization, fractionation, and solidification of the Tuolumne Intrusive Series, Yosemite National Park, California: Geological Society of America Bulletin, v. 90, p. 465–482, doi:10.1130/0016-7606(1979)90<465:CFASOT>2.0.CO;2.

Bateman, P.C., Kistler, R.W., Peck, D.L., and Busacca, A., 1983, Geologic map of the Tuolumne Meadows quadrangle, Yosemite National Park, California: U.S. Geological Survey, GQ-1570, 1:62,500.

Bateman, P.C., Dodge, F.C., and Bruggman, P.E., 1984, Major oxide analyses, CIPW norms, modes, and bulk specific gravities of plutonic rocks from the Mariposa 1 degrees by 2 degrees sheet, central Sierra Nevada, California: U.S. Geological Survey Open-File Report 0196-1497, 59 p.

Chen, W., and Arculus, R.J., 1995, Geochemical and isotopic characteristics of lower crustal xenoliths, San Francisco Volcanic Field, Arizona, U.S.A: Lithos, v. 36, p. 203–225, doi:10.1016/0024-4937(95)00018-6.

Chen, J.H., and Moore, J.G., 1982, Uranium-lead isotopic ages from the Sierra Nevada batholith, California: Journal of Geophysical Research, v. 87, p. 4761–4784, doi:10.1029/JB087iB06p04761.

Clemens, J.D., Helps, P.A., and Stevens, G., 2010, Chemical structure in granitic magmas—A signal from the source?: Transactions of the Royal Society of Edinburgh, v. 100, p. 159–172.

Coleman, D.S., and Glazner, A.F., 1997, The Sierra Crest magmatic event: Rapid formation of juvenile crust during the Late Cretaceous in California: International Geology Review, v. 39, p. 768–787, doi:10.1080/00206819709465302.

Coleman, D.S., Frost, T.P., and Glazner, A.F., 1992, Evidence from the Lamarck Granodiorite for rapid Late Cretaceous crust formation in California: Science, v. 258, p. 1924–1926, doi:10.1126/science.258.5090.1924.

Coleman, D.S., Gray, W., and Glazner, A.F., 2004, Rethinking the emplacement and evolution of zoned plutons: Geochronological evidence for incremental assembly of the Tuolumne Intrusive Suite, California: Geology, v. 32, p. 433–436, doi:10.1130/G20220.1.

Coleman, D.S., Bartley, J.M., Glazner, A.F., and Law, R.D., 2005, Incremental Assembly and Emplacement of Mesozoic Plutons in the Sierra Nevada and White and Inyo Ranges, California: Geological Society of America Field Forum Field Trip Guide (Rethinking the Assembly and Evolution of Plutons: Field Tests and Perspectives, 7–14 October 2005), 59 p.

Columbini, L.L., Miller, C.F., Gualda, G.A.R., Wooden, J.L., and Miller, J.S., 2011, Sphene and zircon in the Highland Range volcanic sequence (Miocene, southern Nevada, USA): Elemental partitioning, phase relations, and influence on evolution of silicic magma: Contributions to Mineralogy and Petrology, v. 102, p. 29–50, doi: 10.1007/s00710-011-0177-3.

Daly, R.A., 1933, Igneous Rocks and the Depths of the Earth: New York, McGraw-Hill, 598 p.

Davis, J.W., Coleman, D.S., Gracely, J.T., Gaschnig, R., and Stearns, M., 2012, Magma accumulation rates and thermal histories of plutons of the Sierra Nevada batholith, California: Contributions to Mineralogy and Petrology, v. 163, no. 3, p. 449–465, doi:10.1007/s00410-011-0683-7.

Economos, R.C., Memeti, V., Paterson, S.R., Miller, J.S., Erdmann, S., and Žák, J., 2010, Causes of compositional diversity in a lobe of the Half Dome granodiorite, Tuolumne Batholih, Central Sierra Nevada, California: Transactions of the Royal Society of Edinburgh, v. 100, p. 173–183.

Eichelberger, J.C., Izbekov, P.E., and Browne, B.L., 2006, Bulk chemical trends at arc volcanoes are not liquid lines of descent: Lithos, v. 87, p. 135–154, doi:10.1016/j.lithos.2005.05.006.

Frost, T.P., and Mahood, G.A., 1987, Field, chemical, and physical constraints on mafic-felsic magma interaction in the Lamarck Granodiorite, Sierra Nevada, California: Geological Society of America Bulletin, v. 99, p. 272–291, doi:10.1130/0016-7606(1987)99<272:FCAPCO>2.0.CO;2.

Glazner, A.F., Bartley, J.M., Coleman, D.S., Gray, W., and Taylor, R.Z., 2004, Are plutons assembled over millions of years by amalgamation from small magma chambers?: GSA Today, v. 14, p. 4–11, doi:10.1130/1052-5173(2004)014<0004:APAOMO>2.0.CO;2.

Glazner, A.F., Coleman, D.S., and Bartley, J.M., 2008, The tenuous connection between high-silica rhyolites and granodiorite plutons: Geology, v. 36, p. 183–186, doi:10.1130/G24496A.1.

Gray, W., Glazner, A.F., Coleman, D.S., and Bartley, J.M., 2008, Long-term geochemical variability of the Late Cretaceous Tuolumne Intrusive Suite, Central Sierra Nevada, California, *in* Annen, C. and Zelmer, G.F., eds., Dynamics of Crustal Magma Transfer, Storage and Differentiation: Geological Society of London, Special Publication, v. 304, p. 183–202.

Hanson, R.B., and Glazner, A.F., 1995, Thermal requirements for extensional emplacement of granitoids: Geology, v. 23, p. 213–216, doi:10.1130/0091-7613(1995)023<0213:TRFEEO>2.3.CO;2.

Higgins, M., 2000, Measurement of crystal size distributions: The American Mineralogist, v. 85, p. 1105–1116.

Hildreth, W., 1981, Gradients in silicic magma chambers: Implications for lithospheric magmatism: Journal of Geophysical Research, v. 86, p. 10,153–10,192, doi:10.1029/JB086iB11p10153.

Hildreth, W., 2004, Volcanological perspectives on Long Valley, Mammoth Mountain, and Mono Craters: Several contiguous but discrete systems: Journal of Volcanology and Geothermal Research, v. 136, p. 169–198, doi:10.1016/j.jvolgeores.2004.05.019.

Hunt, C.P., Moskowitz, B.M., and Banerjee, S.K., 1995, Magnetic properties of rocks and minerals, *in* Ahrens, T.J., ed., Rock Physics and Phase Relations: A handbook of physical constants: American Geophysical Union Reference Shelf, v. 3, p. 189–204.

Johnson, B.R., and Glazner, A.F., 2010, Formation of K-feldspar megacrysts in granodioritic plutons by thermal cycling and late-stage textural coarsening: Contributions to Mineralogy and Petrology, v. 159, p. 599–619, doi:10.1007/s00410-009-0444-z.

Johnson, C.M., Czamanske, G.K., and Lipman, P.W., 1989, Geochemistry of intrusive rocks associated with the Latir volcanic field, New Mexico, and contrasts between evolution of plutonic and volcanic rocks: Contributions to Mineralogy and Petrology, v. 103, p. 90–109, doi:10.1007/BF00371367.

Kistler, R.W., 1973, Geologic map of the Hetch Hetchy Reservoir Quadrangle, Yosemite National Park, California: U.S. Geological Survey Geologic Quadrangle Map GQ-1112.

Kistler, R.W., and Fleck, R.J., 1994, Field guide for a transect of the central Sierra Nevada, California: Geochronology and isotope geology: U.S. Geological Survey Open-File Report 94-267, 53 p.

Kistler, R.W., Chappell, B.W., Peck, D.L., and Bateman, P.C., 1986, Isotopic variation in the Tuolumne intrusive suite, central Sierra Nevada, California: Contributions to Mineralogy and Petrology, v. 94, p. 205–220, doi:10.1007/BF00592937.

Lees, J.M., 2007, Seismic tomography of magmatic systems: Journal of Volcanology and Geothermal Research, v. 167, no. 1–4, p. 37–56, doi:10.1016/j.jvolgeores.2007.06.008.

Lipman, P.W., 1971, Iron-titanium oxide phenocrysts in compositionally zoned ash-flow sheets from southern Nevada: The Journal of Geology, v. 79, p. 438–456, doi:10.1086/627651.

Lipman, P.W., 2007, Incremental assembly and prolonged consolidation of Cordilleran magma chambers: Evidence from the Southern Rocky Mountain volcanic field: Geosphere, v. 3, p. 42–70, doi:10.1130/GES00061.1.

Mahan, K.H., Bartley, J.M., Coleman, D.S., Glazner, A.F., and Carl, B.S., 2003, Sheeted intrusion of the synkinematic McDoogle pluton, Sierra Nevada, California: Geological Society of America Bulletin, v. 115, no. 12, p. 1570–1582, doi:10.1130/B22083.1.

Memeti, V., Patterson, S., and Matzel, J., Mundil, R., and Okaya, D., 2010, Magmatic lobes as "snapshots" of magma chamber growth and evolution in large, composite batholiths: An example from the Tuolumne intrusion, Sierra Nevada, California: Geological Society of America Bulletin, v. 122, p. 1912–1931.

Michael, P., 1984, Chemical differentiation of the Cordillera Paine granite (southern Chile) by in situ fractional crystallization: Contributions to Mineralogy and Petrology, v. 87, p. 179–195, doi:10.1007/BF00376223.

Miller, C.F., and Miller, J.S., 2002, Contrasting stratified plutons exposed in tilt blocks, Eldorado Mountains, Colorado River Rift, Nevada, USA: Lithos, v. 61, p. 209–224, doi:10.1016/S0024-4937(02)00080-4.

Miller, C.F., Furbish, D.J., Walker, B.A., Claiborne, L.L., Koteas, C., Bleick, H.A., and Miller, J.S., 2011, Growth of plutons by incremental emplacement of sheets in crystal rich host: Evidence from Miocene intrusions of the Colorado River region, Nevada, USA: Tectonophysics, v. 500, p. 65–77, doi:10.1016/j.tecto.2009.07.011.

Mills, R.D., Glazner, A.F., and Coleman, D.S., 2008, Comparing the compositional patterns of volcanic and plutonic rocks using the NAVDAT database: Geochimica et Cosmochimica Acta, v. 72, p. A631.

Mills, R.D., Glazner, A.F., and Coleman, D.S., 2009, Scale of pluton/wall rock interaction near May Lake, Yosemite National Park, California, USA: Contributions to Mineralogy and Petrology, v. 158, p. 263–281, doi:10.1007/s00410-009-0381-x.

Moore, J.G., 1963, Geology of the Mount Pinchot Quadrangle southern Sierra Nevada California: U.S. Geological Survey Bulletin 1130, 152 p.

Nakada, S., 1991, Magmatic processes in titanite-bearing dacites, central Andes of Chile and Bolivia: The American Mineralogist, v. 76, p. 548–560.

Paterson, S.R., and Vernon, R.H., 1995, Bursting the bubble of ballooning plutons: A return to nested diapirs emplaced by multiple processes: Geological Society of America Bulletin, v. 107, p. 1356–1380, doi:10.1130/0016-7606(1995)107<1356:BTBOBP>2.3.CO;2.

Pitcher, W.S., and Berger, A.R., 1972, The geology of Donegal: A study of granite emplacement and unroofing: New York, Wiley-Interscience, Regional geology series, 435 p.

Ratajeski, K., Sisson, T.W., and Glazner, A.F., 2005, Experimental and geochemical evidence for derivation of the El Capitan Granite, California, by partial melting of hydrous gabbroic lower crust: Contributions to Mineralogy and Petrology, v. 149, p. 713–734, doi:10.1007/s00410-005-0677-4.

Reid, J.B., Murray, D.P., Hermes, O.D., and Steig, E.J., 1993, Fractional crystallization in granites of the Sierra Nevada: How important is it?: Geology, v. 21, p. 587–590, doi:10.1130/0091-7613(1993)021<0587:FCIGOT>2.3.CO;2.

Sawka, W.N., Chappell, B.W., and Kistler, R.W., 1990, Granitoid compositional zoning by side-wall boundary layer differentiation: Evidence from the Palisade Crest intrusive suite, central Sierra Nevada, California: Journal of Petrology, v. 31, no. 3, p. 519–553.

Sisson, T.W., Grove, T.L., and Coleman, D.S., 1996, Hornblende gabbro sill complex at Onion Valley, California, and a mixing origin for the Sierra Nevada batholith: Contributions to Mineralogy and Petrology, v. 126, p. 81–108, doi:10.1007/s004100050237.

Sisson, T.W., Ratajeski, K., Hankins, W.B., and Glazner, A.F., 2005, Voluminous granitic magmas from common basaltic sources: Contributions to Mineralogy and Petrology, v. 148, p. 635–661, doi:10.1007/s00410-004-0632-9.

Smith, R.L., 1979, Ash-flow magmatism, *in* Chapin, C.E. and Elston, W.E., eds., Ash-Flow Tuffs: Geological Society of America Special Paper 180, p. 5–27.

Solgadi, F., and Sawyer, E.W., 2008, Formation of igneous layering in granodiorite by gravity flow: A field, microstructure and geochemical study of the Tuolumne Intrusive Suite at Sawmill Canyon, California: Journal of Petrology, v. 49, p. 2009–2042, doi:10.1093/petrology/egn056.

Sorensen, S.S., Dunne, G.C., Hanson, R.B., Barton, M.D., Becker, J., Tobisch, O.T., and Fiske, R.S., 1998, From Jurassic shores to Cretaceous plutons: Geochemical evidence for paleoalteration environments of metavolcanic rocks, eastern California: Geological Society of America Bulletin, v. 110, p. 326–343, doi:10.1130/0016-7606(1998)110<0326:FJSTCP>2.3.CO;2.

Stevens, G., Villaros, A., and Moyen, J.F., 2007, Selective peritectic garnet entrainment as the origin of geochemical diversity in S-type granites: Geology, v. 35, p. 9–12, doi:10.1130/G22959A.1.

Tappa, M.J., Coleman, D.S., Mills, R.D., and Samperton, K.M., 2011, The plutonic record of a silicic ignimbrite from the Latir volcanic field, New Mexico: Geochemistry Geophysics Geosystems, v. 12, p. Q10011, doi:10.1029/2011GC003700.

Taylor, R.Z., 2004, Structure and stratigraphy of the May Lake interpluton screen, Yosemite National Park, California [M.S. thesis]: University of North Carolina, Chapel Hill, 55 p.

Verplanck, P.L., Farmer, G.L., McCurry, M., and Mertzman, S.A., 1999, The chemical and isotopic differentiation of an epizonal magma body: Organ Needle Pluton, New Mexico: Journal of Petrology, v. 40, p. 653–678, doi:10.1093/petroj/40.4.653.

Villaros, A., Stevens, G., Moyen, J.-F., and Buick, I.S., 2009, The trace element compositions of S-type granites: Evidence for disequilibrium melting and accessory phase entrainment in the source: Contributions to Mineralogy and Petrology, v. 158, p. 543–561, doi:10.1007/s00410-009-0396-3.

Walker, B.J., Miller, C.F., Claiborne, L.L., Wooden, J.L., and Miller, J.S., 2007, Geology and geochronology of the Spirit Mountain batholith, southern Nevada: Implications for timescales and physical processes of batholith construction: Journal of Volcanology and Geothermal Research, v. 167, p. 239–262, doi:10.1016/j.jvolgeores.2006.12.008.

Wenner, J.M., and Coleman, D.S., 2004, Magma mixing and Cretaceous crustal growth: Geology and geochemistry of granites in the central Sierra Nevada batholith, California: International Geology Review, v. 46, p. 880–903, doi:10.2747/0020-6814.46.10.880.

Wones, D., 1989, Significance of the assemblage titanite + magnetite + quartz in granitic rocks: The American Mineralogist, v. 74, p. 744–749.

Žák, J., and Paterson, S.R., 2005, Characteristics of internal contacts in the Tuolumne Batholith, central Sierra Nevada, California (USA): Implications for episodic emplacement and physical processes in a continental arc magma chamber: Geological Society of America Bulletin, v. 117, p. 1242–1255, doi:10.1130/B25558.1.